Polarization observables in deuteron photodisintegration and electrodisintegration

V. Dmitrasinovic
College of Willam and Mary, Williamsburg, Virginia 23185

Franz Gross
College of Willam and Mary, Williamsburg, Virginia 23185
and Continuous Electron Beam Accelerator Facility, Newport News, Virginia 23606

(Received 7 June 1989)

A comprehensive relativistic treatment of polarization observables in deuteron photo- and electrodisintegration is presented from a unified standpoint. A discussion of necessary and sufficient measurements needed for a complete determination of all transition amplitudes is given.

I. INTRODUCTION

With the construction of new electron accelerator facilities, new types of experiments which can give more detailed knowledge of electronuclear processes will be feasible. In particular, continuous wave (CW) machines make it possible to do coincidence experiments and determine exclusive cross sections. If, in addition, the polarization of the beam, target, or outgoing ejectile is measured, it may be possible to completely determine all of the helicity amplitudes which contribute to the hadronic current, and in this way place strong constraints on any theoretical calculations.

This prospect has aroused new interest in the formalism and theory of coincidence measurements where the polarization of one or several of the particles is measured.[1] In this paper we derive the coincidence cross section for the $d(e,e'p)n$ reaction in the general case when the incoming electron, deuteron target, and one outgoing nucleon are all polarized. There are 162 observables which describe all possible cases, and they are given as bilinear products of the 18 independent amplitudes which completely describe deuteron electrodisintegration. While some of these results have been given previously in nonrelativistic cases,[2] this is the first time, to our knowledge, that all of these observables have been described in a fully relativistic, unified manner. The formulas, summarized in Tables X–XII, will be useful in subsequent calculations. The formulas for deuteron photodisintegration, $\gamma+d\rightarrow p+n$, which is described by only 12 independent amplitudes, are obtained as a natural byproduct of the electrodisintegration results.

Section II contains the derivation of the polarization observables and coincidence cross section. Electrodisintegration is treated in the one-photon exchange approximation as a binary collision of a virtual photon and the deuteron target. The density matrix of the virtual photon is described in terms of the kinematical variables of the electron in the laboratory (lab) system, while the hadronic current can be described in the center-of-mass (c.m.) system of the outgoing nucleon pair, which is a convenient frame in which to present the results for the final state, or to integrate over final-state momenta and convert exclusive cross sections into inclusive cross sections. The density matrices of the deuteron target and the recoiling nucleons are obtained, and their properties under rotations to different coordinate system worked out. First, the structure of the results when expressed in terms of helicity amplitudes is discussed, and then parity conservation is used to simplify (diagonalize) the problem. It is found that the formulas are greatly simplified when a new set of amplitudes is used. These amplitudes, denoted g_i, are similar to transversity amplitudes previously introduced into the study of pion photoproduction[3,4] and discussed by Moravcsik and his collaborators.[5] Finally, the modifications in the formulas required if it is desired to express all variables in the lab system are discussed.

The comparative simplicity of the final results makes it possible to discuss the design of experimental programs of measurements which could, at least in principle, lead to a complete determination of the 18 independent complex amplitudes which describe deuteron electrodisintegration.[6] This requires the measurement of at least 35 quantities (since one overall phase can never be determined). This is discussed in some detail in Sec. III, where one strategy for such a program is presented, and it is shown that *at least one* measurement of a recoil neutron polarization is essential for a program of complete measurements. While such a program may never be carried out, it is still of interest, for planning purposes, to see what kinds of measurements are redundant, and which give truly independent information. These insights can be obtained from the results given in this paper.

This paper contains no dynamical calculations; these are presently under way and will be published elsewhere.

II. FORMALISM

A. The cross-section–electron variables

The Feynman amplitude for the electron scattering process in one-photon exchange approximation, depicted in Fig. 1, is

$$M_{fi}=e^2\bar{u}(k')\gamma_\mu u(k)\frac{D^{\mu\nu}}{q^2}\langle p_1p_2|J_\nu|P_T\rangle$$

$$=\frac{e^2}{q^2}j_\mu D^{\mu\nu}J_\nu\ , \tag{1}$$

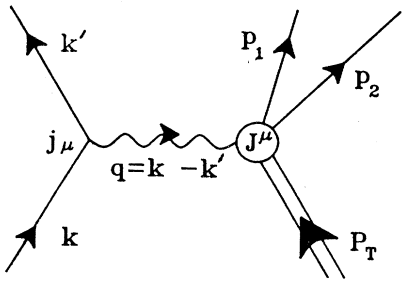

FIG. 1. The Feynman diagram describing deuteron electrodisintegration in the one-photon-exchange approximation.

where j^μ and J^ν are the electron and hadron currents, respectively, $q^\mu=k^\mu-k'^\mu$ is the four momentum transferred by the electron, and the photon projection operator is

$$D^{\mu\nu}=g^{\mu\nu}-\frac{q^\mu q^\nu}{q^2} . \tag{2}$$

Since the currents are conserved,

$$q_\mu j^\mu=0=q_\nu J^\nu , \tag{3}$$

it is customary to drop the $q^\mu q^\nu$ term in $D^{\mu\nu}$. Alternatively, it is convenient to introduce the expansion

$$D^{\mu\nu}=\sum_{\lambda_\gamma}(-1)^{\lambda_\gamma}\epsilon^{\mu *}_{\lambda_\gamma}\epsilon^{\nu}_{\lambda_\gamma} , \tag{4}$$

where the sum is over the photon helicities $\lambda_\gamma=\pm$ or 0, and if the photon momentum is taken to be in the $+\hat{z}$ direction, then in the lab system

$$\begin{aligned}\epsilon^\mu_\pm&=\mp\frac{1}{\sqrt{2}}(0,1,\pm i,0) ,\\ \epsilon^\mu_0&=\left[\frac{q_L}{Q},0,0,\frac{\nu}{Q}\right] ,\end{aligned} \tag{5}$$

where

$$q^\mu=(\nu,0,0,q_L) \tag{6}$$

and $q^2=\nu^2-q_L^2=-Q^2<0$. Note that the polarization vectors have the following properties:

$$\begin{aligned}q_\mu\epsilon^\mu_{\lambda_\gamma}&=0 ,\\ g_{\mu\nu}\epsilon^{\mu *}_{\lambda_\gamma}\epsilon^{\nu}_{\lambda'_\gamma}&=(-1)^{\lambda_\gamma}\delta_{\lambda_\gamma,\lambda'_\gamma} .\end{aligned} \tag{7}$$

The expansion (4) is convenient because it separates the scattering amplitude, defined in Eq. (1), into the sum of products of separately covariant currents

$$M_{fi}=-\sum_{\lambda_\gamma}(-1)^{\lambda_\gamma}\frac{e^2}{Q^2}(j_\mu\epsilon^{\mu *}_{\lambda_\gamma})(J_\nu\epsilon^{\nu}_{\lambda_\gamma}) . \tag{8}$$

In what follows, the electron current will be evaluated in the lab system, and the hadron current in the c.m. system of the outgoing pair of hadrons, with four-momentum p_1 and p_2. This is done in order to simplify the description of the hadronic final state; in particular, with this choice it will be possible to integrate easily over the solid angle of the outgoing hadronic pair and reduce the coincidence cross section to the inclusive cross section. To facilitate this, the cross section is written

$$d^5\sigma=\sum_{\lambda_\gamma\lambda'_\gamma}\frac{e^4}{Q^4}\frac{1}{8EE'M_T}\frac{d^3k'}{(2\pi)^3}(-1)^{\lambda_\gamma-\lambda'_\gamma}L_{\lambda_\gamma\lambda'_\gamma}W_{\lambda_\gamma\lambda'_\gamma} , \tag{9}$$

where E and $E'\gg m$ are the energies of the incoming and outgoing electrons, M_T the mass of the target, and the electron and hadron density matrices are

$$L_{\lambda\lambda'}=\tfrac{1}{2}\mathrm{tr}\{(m+\not k)\not\epsilon_{\lambda'}(m+\not k')\not\epsilon^*_\lambda(1+\gamma^5\not s)\} \tag{10}$$

$$W_{\lambda\lambda'}=\sum_{\text{spins}}\int\frac{d^3p_1d^3p_2}{(2\pi)^6}\frac{M_1M_2}{E_1E_2}(2\pi)^4\times\delta^4(p_1+p_2-P-q)J\cdot\epsilon_\lambda J^\dagger\cdot\epsilon^*_{\lambda'} . \tag{11}$$

The electron density matrix includes the possibility that the incoming electron has spin polarization s^μ satisfying $s\cdot k=0$, and the hadron density matrix implicitly includes spin projection operators as needed to describe the polarization of the initial deuteron, or the polarization of the recoil neutron or proton, or any combination of these. The structure of $W_{\lambda\lambda'}$ will be discussed extensively below—for now we note that it is Lorentz covariant, and hence can be studied in the c.m. system of the outgoing np system, and that in this system the energy-momentum-conserving δ function fixes four of the six integration variables, leaving only the direction of the relative momentum of the final pair $p=\frac{1}{2}(p_1-p_2)$ unspecified. The remainder of this part will be devoted to reducing the electron tensor.

Carrying out the trace in Eq. (10) gives

$$\begin{aligned}L_{\lambda\lambda'}&=2[\,k\cdot\epsilon_\lambda k'\cdot\epsilon^*_\lambda+k\cdot\epsilon^*_\lambda k'\cdot\epsilon_{\lambda'}-(k\cdot k')\epsilon^*_\lambda\cdot\epsilon_{\lambda'}\\ &\quad+2ih\epsilon_{\mu\nu\alpha\beta}\epsilon^{\mu *}_\lambda\epsilon^\nu_{\lambda'}k^\alpha k'^\beta]\\ &=L^0_{\lambda\lambda'}+2hL^h_{\lambda\lambda'} ,\end{aligned} \tag{12}$$

where h is the helicity of the incoming electron, equal to $\pm\frac{1}{2}$, and L is separated into electron-helicity-independent and -dependent terms, L^0 and L^h, respectively. Both parts of L and W (see the next section) are Hermitian

$$\begin{aligned}L_{\lambda\lambda'}&=L^*_{\lambda'\lambda} ,\\ W_{\lambda\lambda'}&=W^*_{\lambda'\lambda} .\end{aligned} \tag{13}$$

The photon polarization vectors (5) satisfy the reflection property

$$\epsilon^{\mu *}_{\lambda\gamma}=(-1)^{\gamma_\lambda}\epsilon^\mu_{-\lambda\gamma} \tag{14}$$

from which it follows that

$$L^{0}_{-\lambda,-\lambda'}=(-1)^{\lambda-\lambda'}L^{0*}_{\lambda\lambda'}\ ,$$
$$L^{h}_{-\lambda,-\lambda'}=(-1)^{1+\lambda-\lambda'}L^{h*}_{\lambda\lambda'}\ . \tag{15}$$

Hence there are only six independent density-matrix elements, as given in Table I. These can be readily evaluated in the lab frame using the explicit forms for the polarization vectors given in Eq. (5). Factoring out a common factor

$$L_{\lambda\lambda'}=4EE'\cos^2\tfrac{1}{2}\theta\ l_{\lambda\lambda'} \tag{16}$$

where θ is the scattering angle of the electron in the lab frame, we choose for these six matrix elements

$$l^0_{00},\ l^0_{0+},\ l^0_{++},\ l^0_{+-},\ l^h_{0+},\ l^h_{++}\ .$$

TABLE I. Relations between the photon density matrix elements. Note that there are only six independent elements.

Unpolarized electrons	Incoming electron with helicity h
l^0_{00}	$l^h_{00}=0$
$l^0_{0+}=-l^{0*}_{0-}=-l^0_{-0}=l^{0*}_{+0}$	$l^h_{0+}=l^{h*}_{0-}=l^h_{-0}=l^{h*}_{+0}$
$l^0_{++}=l^{0*}_{--}$	$l^h_{++}=-l^{h*}_{--}$
$l^0_{+-}=l^{0*}_{-+}$	$l^h_{+-}=l^{h*}_{-+}=0$

Explicit forms for these matrix elements are given in Table II. Note that they are all real. Using Eq. (9), the relations in Table I, and the hermiticity of $W_{\lambda\lambda'}$, gives an intermediate result for the cross section

$$d^5\sigma=\sigma_M\frac{dE'd\Omega'}{4\pi M_T}[\ l^0_{00}W_{00}+l^0_{++}(W_{++}+W_{--})+l^0_{+-}2\,\mathrm{Re}W_{+-}-l^0_{0+}2\,\mathrm{Re}(W_{0+}-W_{0-})$$
$$+2hl^h_{++}(W_{++}-W_{--})-2hl^h_{0+}2\,\mathrm{Re}(W_{0+}+W_{0-})]\ , \tag{17}$$

where

$$\sigma_M=\left[\frac{\alpha\cos\frac{1}{2}\theta}{2E\sin^2\frac{1}{2}\theta}\right]^2\ . \tag{18}$$

To reduce the cross section further, we study the hadronic density matrix $W_{\lambda\lambda'}$ in the next section.

B. The cross-section–hadron variables

The hadronic density matrix was defined in Eq. (11). It is explicitly Lorentz covariant, and can therefore be evaluated in any frame. The kinematics of the lab frame for the entire scattering process are shown in Fig. 2. The struck hadron (which has four-momentum p_1 by convention) emerges at an angle θ_1 with respect to the direction of the photon's three momentum, $\mathbf{q}$, and lies in a plane tilted with respect to the electron scattering plane by an angle ϕ as shown. If $\phi\neq 0$ or π, the exclusive process is referred to as "out of plane."

It is convenient to evaluate $W_{\lambda\lambda'}$ in the c.m. frame of the outgoing hadronic pair p_1 and p_2, and to work in a coordinate system where $\mathbf{p}_1$ lies in the x-z plane. The reason for choosing to work in this coordinate system is that it corresponds to the conventional choice for descriptions of two-body scattering processes, and we may therefore carry over all of the standard conventions. The new x-z plane is referred to as the ejectile plane, and is tilted at the angle ϕ with respect to the electron plane as shown in Fig. 2. The axes of this new plane are labeled (x',y',z'). Because $W_{\lambda\lambda'}$ is covariant, it may be evaluated directly in this coordinate system without the need for special transformations.

However, one delicacy must be handled carefully. The photon helicity vectors (5) were prepared in the lab electron scattering plane, and must be explicitly related to helicity vectors appropriate to the c.m. ejectile scattering plane. The transformation which carries one from the (x,y,z) system to the (x',y',z') system is a pure boost in the $+\hat{z}$ direction, followed by a rotation through angle

TABLE II. Explicit forms for the six independent $l_{\lambda\lambda'}$, introduced in Sec. II A, are given in the right-hand column. They are also related to the $v_i's$ introduced by Donnelly (Ref. 1).

$l^0_{00}=\dfrac{Q^2}{q_L^2}$	$\rho_{00}=\left[\dfrac{W}{M_T}\dfrac{Q}{q_L}\right]^2 l^0_{00}=\left[\dfrac{W}{M_T}\right]^2 v_L$
$l^0_{0+}=\dfrac{1}{\sqrt{2}}\dfrac{Q}{q_L}\left[\dfrac{Q^2}{q_L^2}+\tan^2\dfrac{1}{2}\theta\right]^{1/2}$	$\rho_{0+}=\left[\dfrac{W}{M_T}\dfrac{Q}{q_L}\right]l^0_{0+}=-\dfrac{W}{M_T}v_{TL}$
$l^0_{++}=\dfrac{1}{2}\dfrac{Q^2}{q_L^2}+\tan^2\dfrac{1}{2}\theta$	$\rho_{++}=l^0_{++}=v_T$
$l^0_{+-}=-\dfrac{Q^2}{2q_L^2}$	$\rho_{+-}=l^0_{+-}=v_{TT}$
$l^h_{0+}=\dfrac{1}{\sqrt{2}}\dfrac{Q}{q_L}\tan\dfrac{1}{2}\theta$	$\rho'_{0+}=\left[\dfrac{W}{M_T}\dfrac{Q}{q_L}\right]l^h_{0+}=-\dfrac{W}{M_T}v'_{TL}$
$l^h_{++}=\tan\dfrac{1}{2}\theta\left[\dfrac{Q^2}{q_L^2}+\tan^2\dfrac{1}{2}\theta\right]^{1/2}$	$\rho'_{++}=l^h_{++}=v'_T$

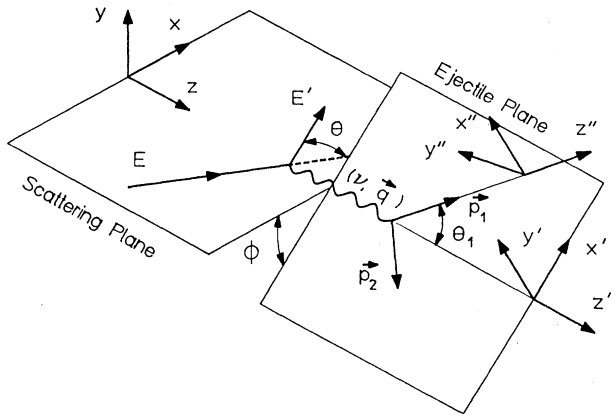

FIG. 2. Diagram of the electrodisintegration process showing the electron scattering plane, the ejectile plane, and the two coordinate systems in the ejectile plane: (x',y',z') and (x'',y'',z'').

$+\phi$ about the $\hat{z}$ axis. The boost is defined by the requirement that the three momentum of the final state with four momentum $P=p_1+p_2$ be brought to zero. If W is the invariant mass of the final state, then in the lab system

$$P_L^\mu=[(W^2+q_L^2)^{1/2},0,0,q_L] \tag{19}$$

and in the c.m. system, $P^\mu_{\text{c.m.}}=(W,\mathbf{0})$. Hence the boost transformation is, in matrix form,

$$B_{\text{c.m.}}=\begin{bmatrix} \frac{(W^2+q_L^2)^{1/2}}{W} & 0 & 0 & \frac{-q_L}{W} \\ 0 & 1 & 0 & 0 \\ 0 & 0 & 1 & 0 \\ \frac{-q_L}{W} & 0 & 0 & \frac{(W^2+q_L^2)^{1/2}}{W} \end{bmatrix} \tag{20}$$

so that if $q^\mu_{\text{c.m.}}=(\nu_0,0,0,q_0)$, then

$$q_0=\frac{(W^2+q_L^2)^{1/2}}{W}q_L-\frac{q_L}{W}\nu=\frac{M_T}{W}q_L\ . \tag{21}$$

The transverse helicity amplitudes are unchanged by the boost, and ϵ_0 has the same form as in Eq. (5) with q_0 and ν_0 replacing q_L and ν.

The rotation through ϕ about the z axis leaves the longitudinal polarization vector unchanged, but changes the phase of the transverse components. The transformed polarization vectors, $\epsilon'_\pm$, become

$$\epsilon'_\pm=e^{\mp i\phi}\epsilon_\pm\ , \tag{22}$$

where $\epsilon_\pm$ are the conventional vectors defined in Eq. (5). Hence, the overall effect of the transformation from the lab electron plane to the c.m. ejectile plane is to modify $W_{\lambda\lambda'}$ as follows:

$$W'_{\lambda\lambda'}=e^{-i\phi(\lambda-\lambda')}W_{\lambda\lambda'}\ . \tag{23}$$

Inverting this expression gives

$$W_{\lambda\lambda'}=e^{+i\phi(\lambda-\lambda')}W'_{\lambda\lambda'}\ . \tag{24}$$

This phase introduces a nontrivial ϕ dependence into the total cross section. Substituting (24) into (17) permits us to extract this ϕ dependence, giving

$$\begin{aligned} d^5\sigma=\sigma_M\frac{dE'd\Omega'}{4\pi M_T}[\ & l^0_{00}W'_{00}+l^0_{++}(W'_{++}+W'_{--})+l^0_{+-}\cos2\phi\ 2\,\mathrm{Re}W'_{+-}-l^0_{+-}\sin2\phi\ 2\,\mathrm{Im}W'_{+-} \\ & -l^0_{0+}\cos\phi\ 2\,\mathrm{Re}(W'_{0+}-W'_{0-})-l^0_{0+}\sin\phi\ 2\,\mathrm{Im}(W'_{0+}+W'_{0-}) \\ & +2hl^h_{++}(W'_{++}-W'_{--})-2hl^h_{0+}\cos\phi\ 2\,\mathrm{Re}(W'_{0+}+W'_{0-})-2hl^h_{0+}\sin\phi\ 2\,\mathrm{Im}(W'_{0+}-W'_{0-})]\ . \end{aligned} \tag{25}$$

This form of the cross section displays the exact ϕ dependence, provided any polarization vectors which enter $W'_{\lambda\lambda'}$ are defined with respect to the $(x'y'z')$ coordinate system.

The next step in obtaining the coincidence cross section is to carry out the integrals in Eq. (11) in the c.m. frame. This gives

$$W'_{\lambda\lambda'}=d\Omega_1 p_1 R_{\lambda\lambda'} \tag{26}$$

where, if $\kappa^2=M_1M_2/4\pi^2W$,

$$R_{\lambda\lambda'}=\kappa^2\sum_s J'\cdot\epsilon_\lambda J'^{\,\dagger}\cdot\epsilon^*_{\lambda'}=\kappa^2\sum_s J_\lambda J^\dagger_{\lambda'}\ , \tag{27}$$

where we use the notation $J_\lambda=J'\cdot\epsilon_\lambda$. It is quite common to use current conservation to express the longitudinal hadronic current in terms of its J^0 component. This reduction is not frame independent. If used, it should be carried out in the frame in which J is to be evaluated (the c.m. frame). In this frame

$$q'_\mu J'^{\,\mu}=\nu_0 J'^{\,0}-q_0 J'^{\,3}=0\ . \tag{28}$$

Hence

$$\begin{aligned} J_0=\epsilon'^\mu_0 J'_\mu&=\frac{q_0}{Q}J'^{\,0}-\frac{\nu_0}{Q}J'^{\,3} \\ &=\frac{Q}{q_0}J'^{\,0}=\left[\frac{W}{M_T}\frac{Q}{q_L}\right]J'^{\,0}=\left[\frac{1}{\eta}\right]J'^{\,0}\ , \end{aligned} \tag{29}$$

where Eq. (21) was used in the final step. If 0 appears as a superscript, it will refer to the time component of the current, and not the longitudinal helicity, and an extra

factor of $1/\eta=[(W/M_T)(Q/q_L)]$ must accompany each such superscript. Density matrices with these extra factors, $\rho_{\lambda\lambda'}$, were defined in Table II. Because this convention has become quite familiar, we will present results in terms of these density matrices, and correct for the factors $1/\eta$ by adding factors of η to the corresponding structure functions (see Table III).

Combining Eq. (25), (26), and (27) and using Table II gives us our general form for the coincidence cross section:

$$\frac{d^5\sigma}{d\Omega' dE' d\Omega_1}=\frac{\sigma_M p_1}{4\pi M_T}\left\{\left[\frac{W}{M_T}\right]^2 v_L R_L+v_T R_T+v_{TT}[\cos 2\phi R_{TT}^{(\mathrm{I})}+\sin 2\phi R_{TT}^{(\mathrm{II})}]\right.$$
$$\left.+\left[\frac{W}{M_T}\right]v_{TL}[\cos\phi R_{LT}^{(\mathrm{I})}+\sin\phi R_{LT}^{(\mathrm{II})}]+2hv'_T R_{T'}+2h\left[\frac{W}{M_T}\right]v'_{TL}[\cos\phi R_{LT'}^{(\mathrm{II})}+\sin\phi R_{LT'}^{(\mathrm{I})}]\right\}. \quad (30)$$

The relationships between the R's introduced in this expression and the covariant R's of Eq. (27) are given in Table III.

Our results agree with those previously obtained by Walecka and Zucker.[7] However, previous derivations of this cross section given by Arenhovel[8] have omitted the factors of W/M_T associated with the transformation (29), although they are included in Ref. 2. (Note that these factors do not occur if the hadronic current is evaluated in the lab frame—see Sec. II H.) Since these derivations treated the hadronic currents nonrelativistically, and these factors are of relativistic origin, it could be argued that they may be neglected. We believe that even if the currents are calculated nonrelativistically, such kinematic factors should be regarded as part of the cross section and should not be neglected. For light targets, such as the deuteron, they are not small. For example, for $Q^2=1(\mathrm{GeV}/c)^2$ at the quasielastic peak, where $x\equiv Q^2/2M\nu=1$,

$$\frac{W}{M_T}=\left[1+\frac{Q^2}{M_T^2}\left[\frac{M_T}{Mx}-1\right]\right]^{1/2}\simeq 1+\frac{Q^2}{2M_T^2}\simeq 1.16\ , \quad (31)$$

which gives an enhancement of approximately 16%. It is very important to treat such factors systematically and consistently.

TABLE III. The R's used in Eq. (30) (left-hand column) are equal to expressions involving $R_{\lambda\lambda'}$ [defined in Eq. (27)] given in the center column, or the sums over current operators given in the right-hand column. In the right-hand column, $J_\pm=J'\cdot\epsilon_\pm$ but $J^0=J'^0$ as defined in Eq. (29). Note that, because of the metric tensor, $J_\pm=\pm(1/\sqrt{2})(J_x\pm iJ_y)$, which is opposite in sign from that used in Refs. 3 and 7. Our overall results agree with these references.

R_L	$\eta^2 R_{00}$	$\kappa^2\sum\lvert J^0\rvert^2$
R_T	$R_{++}+R_{--}$	$\kappa^2\sum(\lvert J_+\rvert^2+\lvert J_-\rvert^2)$
$R_{TT}^{(\mathrm{I})}$	$2\,\mathrm{Re}R_{+-}$	$2\kappa^2\mathrm{Re}\sum(J_+J_-^\dagger)$
$R_{TT}^{(\mathrm{II})}$	$-2\,\mathrm{Im}R_{+-}$	$-2\kappa^2\mathrm{Im}\sum(J_+J_-^\dagger)$
$R_{LT}^{(\mathrm{I})}$	$2\eta\,\mathrm{Re}(R_{0+}-R_{0-})$	$2\kappa^2\mathrm{Re}\sum J^0(J_+^\dagger-J_-^\dagger)$
$R_{LT}^{(\mathrm{II})}$	$2\eta\,\mathrm{Im}(R_{0+}+R_{0-})$	$2\kappa^2\mathrm{Im}\sum J^0(J_+^\dagger+J_-^\dagger)$
$R_{T'}$	$R_{++}-R_{--}$	$\kappa^2\sum(\lvert J_+\rvert^2-\lvert J_-\rvert^2)$
$R_{LT'}^{(\mathrm{II})}$	$2\eta\,\mathrm{Re}(R_{0+}+R_{0-})$	$2\kappa^2\mathrm{Re}\sum J^0(J_+^\dagger+J_-^\dagger)$
$R_{LT'}^{(\mathrm{I})}$	$2\eta\,\mathrm{Im}(R_{0+}-R_{0-})$	$2\kappa^2\mathrm{Im}\sum J^0(J_+^\dagger-J_-^\dagger)$

C. The cross section for polarized hadrons—general formulas

The sums over hadron spin states which appear in the spectral functions defined in Table III must still be specified more completely. If the hadrons are completely unpolarized, the generic term Eq. (27) is

$$R_{ab}=\kappa^2\sum J_a J_b^\dagger$$
$$=\frac{\kappa^2}{3}\sum_{\lambda_d\lambda_1\lambda_2}\langle\lambda_1\lambda_2|J_a|\lambda_d\rangle\langle\lambda_d|J_b^\dagger|\lambda_1\lambda_2\rangle\ , \quad (32)$$

where we have averaged over the polarization states of the deuteron and summed over the polarization states of the two outgoing nucleons. In matrix form, $\langle\lambda_1\lambda_2|J_a|\lambda_d\rangle$ is a 4×3 matrix, and (32) can be written simply as

$$R_{ab}=\frac{\kappa^2}{3}\mathrm{tr}\{\hat{J}_a\hat{J}_b^\dagger\}\ . \quad (33)$$

In general, the target or either of the two hadrons may be polarized, and the polarization can be described using a density matrix ρ_D or ρ_N. The generalized expression which allows for this possibility is

$$R_{ab}=4\kappa^2\mathrm{tr}\{\rho_N\hat{J}_a\rho_D\hat{J}_b^\dagger\}\ , \quad (34)$$

where the density matrices for nucleons and deuterons are normalized to $\mathrm{tr}(\rho)=1$. The remaining task is to describe these density matrices, and to simplify the expressions.

1. Deuteron polarization

The polarization state of the deuteron is described by a spin-1 density matrix. As a consequence of its hermiticity and the normalization condition (trace=1), this matrix is specified by eight real parameters. In the Cartesian representation these are the three components of the polarization vector P_i and five components of the (symmetric) polarization tensor P_{ij}. In the spherical basis they are three rank-1 and five rank-2 tensors: T_{1M} and T_{2M}. We follow the notation of Ohlsen.[9] These quantities are defined via the (ensemble) average values of the spin-1 operators S_i and S_{ij}, where

$$S_{ij}=\tfrac{3}{2}(S_iS_j+S_jS_i)-2\delta_{ij}\ . \quad (35)$$

In the spherical basis, spanned by (ξ_+,ξ_0,ξ_-) where $\xi_\pm=\mp(1/\sqrt{2})(1,\pm i,0)$ and $\xi_0=(0,0,1)$, these spin-1 operators assume the following familiar form:

$$S_x=\frac{1}{\sqrt{2}}\begin{bmatrix}0&1&0\\1&0&1\\0&1&0\end{bmatrix},\quad S_y=\frac{i}{\sqrt{2}}\begin{bmatrix}0&-1&0\\1&0&-1\\0&1&0\end{bmatrix},\quad S_z=\begin{bmatrix}1&0&0\\0&0&0\\0&0&-1\end{bmatrix}. \tag{36}$$

The spin-1 density matrix ρ_D can be written in the form

$$\rho_D=\tfrac{1}{3}\left[1+\tfrac{3}{2}\mathbf{S}\cdot\mathbf{P}+\tfrac{2}{3}\sum_{i<j}S_{ij}P_{ij}+\tfrac{1}{2}S_{zz}P_{zz}+\tfrac{1}{6}(S_{xx}-S_{yy})(P_{xx}-P_{yy})\right]. \tag{37}$$

The density matrix ρ_D can also be expanded in terms of spherical irreducible tensor operators of rank 0, 1, and 2:

$$\rho_D=\tfrac{1}{3}\sum_{J=0}^{2}\sum_{M=-J}^{J}\tilde{T}^{*}_{JM}\tau_{JM}\ , \tag{38}$$

where

$$\begin{aligned}\tau^{\dagger}_{JM}&=(-1)^M\tau_{J-M}\ ,\\ \tilde{T}^{*}_{JM}&=(-1)^M\tilde{T}_{J-M}\ ,\end{aligned} \tag{39}$$

and the relations between the τ's and S's (or $\tilde{T}$'s and P's) are given in Table IV. Using these definitions, and Eqs. (35) and (36), we can write the density matrix as

$$\rho_D=\frac{1}{3}\begin{bmatrix}1+\sqrt{\tfrac{3}{2}}\tilde{T}_{10}+\frac{1}{\sqrt{2}}\tilde{T}_{20} & -\sqrt{\tfrac{3}{2}}(\tilde{T}^{*}_{11}+\tilde{T}^{*}_{21}) & \sqrt{3}\tilde{T}^{*}_{22}\\ -\sqrt{\tfrac{3}{2}}(\tilde{T}_{11}+\tilde{T}_{21}) & 1-\sqrt{2}\tilde{T}_{20} & -\sqrt{\tfrac{3}{2}}(\tilde{T}^{*}_{11}-\tilde{T}^{*}_{21})\\ \sqrt{3}\tilde{T}_{22} & -\sqrt{\tfrac{3}{2}}(\tilde{T}_{11}-\tilde{T}_{21}) & 1-\sqrt{\tfrac{3}{2}}\tilde{T}_{10}+\frac{1}{\sqrt{2}}\tilde{T}_{20}\end{bmatrix}, \tag{40}$$

where use was made of the symmetry relations (39) for $\tilde{T}_{JM}$. This matrix is with respect to the standard ξ_+,ξ_0,ξ_- basis, which is appropriate for deuteron polarizations defined with respect to the (x',y',z') coordinate system shown in Fig. 2 (where the z' axis is in the direction of the three momentum carried by the photon, $\mathbf{q}$).

In what follows, we will use the helicity formalism for the hadronic particles. Following the standard conventions,[10] the deuteron will be taken to be particle number 2 in the initial state, and its helicity vectors are therefore obtained from the standard ξ_λ's according to

$$\tilde{\xi}_{\lambda_d}=(-1)^{1-\lambda_d}e^{-i\pi S_y}\xi_{\lambda_d}=A\,\xi_{\lambda_d}\ . \tag{41}$$

The transformation matrix A in the spherical basis is

$$A=\begin{bmatrix}0&0&1\\0&1&0\\1&0&0\end{bmatrix}=A^{\dagger}=A^{-1}\ , \tag{42}$$

which gives the relation

$$\tilde{\xi}_{\lambda_d}=\xi_{-\lambda_d}\ . \tag{43}$$

In this new, helicity basis, the density matrix ρ_D becomes

$$\tilde{\rho}_D=\frac{1}{3}\begin{bmatrix}1-\sqrt{\tfrac{3}{2}}\tilde{T}_{10}+\frac{1}{\sqrt{2}}\tilde{T}_{20} & -\sqrt{\tfrac{3}{2}}(\tilde{T}_{11}-\tilde{T}_{21}) & \sqrt{3}\tilde{T}_{22}\\ -\sqrt{\tfrac{3}{2}}(\tilde{T}^{*}_{11}-\tilde{T}^{*}_{21}) & 1-\sqrt{2}\tilde{T}_{20} & -\sqrt{\tfrac{3}{2}}(\tilde{T}_{11}+\tilde{T}_{21})\\ \sqrt{3}\tilde{T}^{*}_{22} & -\sqrt{\tfrac{3}{2}}(\tilde{T}^{*}_{11}+\tilde{T}^{*}_{21}) & 1+\sqrt{\tfrac{3}{2}}\tilde{T}_{10}+\frac{1}{\sqrt{2}}\tilde{T}_{20}\end{bmatrix}. \tag{44}$$

TABLE IV. Definitions of the operators τ_{JM} in terms of the spin-one operators S_i and S_{ij} given in Eqs. (35) and (36). Precisely the same equations relate the $\tilde{T}_{JM}$ of Eq. (40) to the P_i and P_{ij}.

Rank 0	$\tau_{00}=1$
Rank 1	$\tau_{1\pm1}=\mp\frac{\sqrt{3}}{2}(S_x\pm iS_y)$
	$\tau_{10}=\sqrt{\frac{3}{2}}S_z$
Rank 2	$\tau_{2\pm2}=\frac{1}{2\sqrt{3}}(S_{xx}-S_{yy}\pm 2iS_{xy})$
	$\tau_{2\pm1}=\mp\frac{1}{\sqrt{3}}(S_{xz}\pm iS_{yz})$
	$\tau_{20}=\frac{1}{\sqrt{2}}S_{zz}$

This matrix gives the deuteron polarization observables *defined with respect to the primed coordinate system* in terms of deuteron helicity states $\tilde{\xi}_{\lambda_d}$, and is the one appropriate to our calculation. Note that the relations (39) insure that this matrix is Hermitian.

2. Nucleon polarization

The density matrices for the outgoing nucleons, normalized so $\mathrm{tr}\rho=1$, are easily constructed from the familiar spin-$\frac{1}{2}$ projection operators.

$$\rho_p=\tfrac{1}{2}(1+\sigma\cdot P)=\frac{1}{2}\begin{bmatrix}1+P_z & P_x-iP_y\\ P_x+iP_y & 1-P_z\end{bmatrix}. \tag{45}$$

We will choose the proton to be particle 1, and the neutron particle 2 (in the sense of Jacob and Wick), and will define the polarizations with respect to the (x'',y'',z'') system shown in Fig. 2. Later on, we will use the standard notation s, n, and l to denote proton polarizations in the x'', y'', and z'' directions, respectively. The proton is traveling in the $+z''$ direction, and the neutron, in the c.m. of the outgoing pair, in the $-z''$ direction. In this case the matrix in Eq. (45) is already in the correct form to use with both the proton and neutron helicity amplitudes, *provided we remember that $P_z=1$ for the proton corresponds to polarization in the $+z''$ direction, while $P_z=1$ for the neutron corresponds to polarization in the $-z''$ direction.* We will adopt this convention here. If it is desired to express the neutron polarization directly in terms of the (x'',y'',z'') coordinate system, the connection is

$$\begin{aligned}\tilde{\chi}_{\lambda n}&=(-1)^{1/2-\lambda_n}e^{-i\pi(\sigma_y/2)}\chi_{\lambda n}\\ &=\sigma_x\chi_{\lambda n}=\chi_{-\lambda n}\end{aligned} \tag{46}$$

and the formulas we obtain can be converted to this convention by changing $P_z\rightarrow -P_z$ and $P_y\rightarrow -P_y$, while leaving P_x unchanged.

If the proton and neutron helicities states are represented by a four-component vector V_i with components

$$\begin{aligned}V_1&=|++\rangle,\quad V_2=|+-\rangle,\\ V_3&=|-+\rangle,\quad V_4=|--\rangle\end{aligned} \tag{47}$$

where the first entry is the helicity of the proton, the nucleon density matrix becomes

$$\rho_N=\frac{1}{4}\begin{bmatrix}(1+P_z)(1+P_z') & (1+P_z)(P_x'-iP_y') & (P_x-iP_y)(1+P_z') & (P_x-iP_y)(P_x'-iP_y')\\ (1+P_z)(P_x'+iP_y') & (1+P_z)(1-P_z') & (P_x-iP_y)(P_x'+iP_y') & (P_x-iP_y)(1-P_z')\\ (P_x+iP_y)(1+P_z') & (P_x+iP_y)(P_x'-iP_y') & (1-P_z)(1+P_z') & (1-P_z)(P_x'-iP_y')\\ (P_x+iP_y)(P_x'+iP_y') & (P_x+iP_y)(1-P_z') & (1-P_z)(P_x'+iP_y') & (1-P_z)(1-P_z')\end{bmatrix}, \tag{48}$$

where P and P' are the polarizations of the outgoing proton and neutron, respectively, *defined with respect to the (x'',y'',z'') coordinate system for the proton, and the $(x'',-y'',-z'')$ coordinate system for the neutron.* This is the density matrix we will use. Note that it is Hermitian. We now turn to the specification of the matrix elements of the current.

D. Polarization observables in helicity basis

For electrodisintegration, there are 36 helicity amplitudes, but parity conservation can be used to express 18 of them in terms of the other 18 through the relation

$$\begin{aligned}&\langle-\lambda_p,-\lambda_n|J_{-\lambda_\gamma}|-\lambda_D\rangle\\ &\quad=\eta_g(-1)^{\lambda_p-\lambda_n-(\lambda_\gamma-\lambda_D)}\langle\lambda_p\lambda_n|J_{\lambda_\gamma}|\lambda_D\rangle\end{aligned} \tag{49}$$

where, for deuteron electrodisintegration

$$\eta_g=\eta(-1)^{s_\gamma+s_D-s_p-s_n}=1, \tag{50}$$

where η is the product of the intrinsic parities of the four particles, and s_i are the spins. (Note that Ref. 6 contains an error;[11] it is assumed there that $\eta_g=-1$ instead of $+1$.) The relation (49) follows from the transformation $Y=e^{-i\pi J_y}\hat{P}$, which has the same effect as inversion in the x-z plane. The 18 independent helicity amplitudes are labeled using the convention introduced by Renard *et al.*[6]

$$
\begin{aligned}
&F_{1,2}=\langle \pm\tfrac{1}{2}\pm\tfrac{1}{2}|J\cdot\epsilon_+|1\rangle,\quad F_{3,4}=\langle \pm\tfrac{1}{2}\pm\tfrac{1}{2}|J\cdot\epsilon_+|0\rangle\ ,\\
&F_{5,6}=\langle \pm\tfrac{1}{2}\pm\tfrac{1}{2}|J\cdot\epsilon_+|-1\rangle,\quad F_{7,8}=\langle \pm\tfrac{1}{2}\mp\tfrac{1}{2}|J\cdot\epsilon_+|1\rangle\ ,\\
&F_{9,10}=\langle \pm\tfrac{1}{2}\mp\tfrac{1}{2}|J\cdot\epsilon_+|0\rangle,\quad F_{11,12}=\langle \pm\tfrac{1}{2}\mp\tfrac{1}{2}|J\cdot\epsilon_+|-1\rangle\ ,\\
&F_{13,15}=\langle \tfrac{1}{2}\tfrac{1}{2}|J\cdot\epsilon_0|\pm1\rangle,\quad F_{14}=\langle \tfrac{1}{2}\tfrac{1}{2}|J\cdot\epsilon_0|0\rangle\ ,\\
&F_{16,18}=\langle -\tfrac{1}{2}\tfrac{1}{2}|J\cdot\epsilon_0|\pm1\rangle,\quad F_{17}=\langle -\tfrac{1}{2}\tfrac{1}{2}|J\cdot\epsilon_0|0\rangle\ .
\end{aligned}
\tag{51}
$$

In matrix form this gives

$$
\tilde{J}_+=\begin{bmatrix} F_1 & F_3 & F_5 \\ F_7 & F_9 & F_{11} \\ F_8 & F_{10} & F_{12} \\ F_2 & F_4 & F_6 \end{bmatrix},\quad
\tilde{J}_0=\begin{bmatrix} F_{13} & F_{14} & F_{15} \\ F_{18} & -F_{17} & F_{16} \\ F_{16} & F_{17} & F_{18} \\ -F_{15} & F_{14} & -F_{13} \end{bmatrix},\quad
\tilde{J}_-=\begin{bmatrix} F_6 & -F_4 & F_2 \\ -F_{12} & F_{10} & -F_8 \\ -F_{11} & F_9 & -F_7 \\ F_5 & -F_3 & F_1 \end{bmatrix}\ .
\tag{52}
$$

Note that the Y parity constraints (49) take on a simple form in this matrix space. Specifically,

$$
\tilde{Y}_4\tilde{J}_a\tilde{Y}_3=\eta_\gamma(-1)^{1-a}\tilde{J}_{-a}\ ,
\tag{53}
$$

where $\eta_\gamma=-1$ is the intrinsic parity of the photon, and the intrinsic parities and phases of the nucleons are incorporated into $\tilde{Y}_4$ and of the deuteron into $\tilde{Y}_3$,

$$
\tilde{Y}_4=\eta_p\eta_n\begin{bmatrix} 0 & 0 & 0 & -1 \\ 0 & 0 & 1 & 0 \\ 0 & 1 & 0 & 0 \\ -1 & 0 & 0 & 0 \end{bmatrix},\quad
\tilde{Y}_3=\eta_D\begin{bmatrix} 0 & 0 & 1 \\ 0 & -1 & 0 \\ 1 & 0 & 0 \end{bmatrix},
\tag{54}
$$

where $\eta_p=\eta_n=\eta_D=1$, and $\tilde{Y}_i^{\,2}=1$.

It will be convenient to introduce density matrices which are even or odd under Y parity. If $\alpha=\pm1$, the combinations

$$
\begin{aligned}
&\tilde{\rho}_N^{\,\alpha}=\tfrac{1}{2}(\rho_N+\alpha\tilde{Y}_4\rho_N\tilde{Y}_4)\ ,\\
&\tilde{\rho}_D^{\,\alpha}=\tfrac{1}{2}(\tilde{\rho}_D+\alpha\tilde{Y}_3\tilde{\rho}_D\tilde{Y}_3)
\end{aligned}
\tag{55}
$$

transform like

$$
\begin{aligned}
&\tilde{\rho}_N^{\,\alpha}=\alpha\tilde{Y}_4\tilde{\rho}_N^{\,\alpha}\tilde{Y}_4\ ,\\
&\tilde{\rho}_D^{\,\alpha}=\alpha\tilde{Y}_3\tilde{\rho}_D^{\,\alpha}\tilde{Y}_3\ .
\end{aligned}
\tag{56}
$$

It is straightforward to show, neglecting all terms which depend on the products of P_iP_j' (because the case of *both* nucleons polarized in the final state will not be considered in this paper), that

$$
\begin{aligned}
&\tilde{\rho}_N^{\,+}=\frac{1}{4}\begin{bmatrix} 1 & -iP_y' & -iP_y & 0 \\ iP_y' & 1 & 0 & -iP_y \\ iP_y & 0 & 1 & -iP_y' \\ 0 & iP_y & iP_y' & 1 \end{bmatrix},\\
&\tilde{\rho}_N^{\,-}=\frac{1}{4}\begin{bmatrix} P_z+P_z' & P_x' & P_x & 0 \\ P_x' & P_z-P_z' & 0 & P_x \\ P_x & 0 & -P_z+P_z' & P_x' \\ 0 & P_x & P_x' & -P_z-P_z' \end{bmatrix}
\end{aligned}
\tag{57}
$$

and

$$\tilde{\rho}_D^{+}=\frac{1}{3}\begin{bmatrix} 1+\frac{1}{\sqrt{2}}\tilde{T}_{20} & \sqrt{\frac{3}{2}}(\mathrm{Re}\tilde{T}_{21}-i\,\mathrm{Im}\tilde{T}_{11}) & \sqrt{3}\,\mathrm{Re}\tilde{T}_{22} \\ \sqrt{\frac{3}{2}}(\mathrm{Re}\tilde{T}_{21}+i\,\mathrm{Im}\tilde{T}_{11}) & 1-\sqrt{2}\tilde{T}_{20} & -\sqrt{\frac{3}{2}}(\mathrm{Re}\tilde{T}_{21}+i\,\mathrm{Im}\tilde{T}_{11}) \\ \sqrt{3}\,\mathrm{Re}\tilde{T}_{22} & -\sqrt{\frac{3}{2}}(\mathrm{Re}\tilde{T}_{21}-i\,\mathrm{Im}\tilde{T}_{11}) & 1+\frac{1}{\sqrt{2}}\tilde{T}_{20} \end{bmatrix},$$

$$\tilde{\rho}_D^{-}=\frac{1}{3}\begin{bmatrix} -\sqrt{\frac{3}{2}}\tilde{T}_{10} & -\sqrt{\frac{3}{2}}(\mathrm{Re}\tilde{T}_{11}-i\,\mathrm{Im}\tilde{T}_{21}) & i\sqrt{3}\,\mathrm{Im}\tilde{T}_{22} \\ -\sqrt{\frac{3}{2}}(\mathrm{Re}\tilde{T}_{11}+i\,\mathrm{Im}\tilde{T}_{21}) & 0 & -\sqrt{\frac{3}{2}}(\mathrm{Re}\tilde{T}_{11}+i\,\mathrm{Im}\tilde{T}_{21}) \\ -i\sqrt{3}\,\mathrm{Im}\tilde{T}_{22} & -\sqrt{\frac{3}{2}}(\mathrm{Re}\tilde{T}_{11}-i\,\mathrm{Im}\tilde{T}_{21}) & \sqrt{\frac{3}{2}}\tilde{T}_{10} \end{bmatrix}. \tag{58}$$

The new density matrices $\tilde{\rho}_N^{\alpha}$ and $\tilde{\rho}_D^{\alpha}$ simplify the analysis. To see how this works, introduce new R matrices constructed from these density matrices

$$R_{ab}^{\alpha\beta}=4\kappa^2\mathrm{tr}\{\tilde{\rho}_N^{\alpha}\tilde{J}_a\tilde{\rho}_D^{\beta}J_b^{\dagger}\}\ . \tag{59}$$

These now have simple symmetry properties, which follow from the Y parity transformations (53) and (56),

$$R_{ab}^{\alpha\beta}=\alpha\beta(-1)^{a+b}R_{-a-b}^{\alpha\beta}\ , \tag{60}$$

and the original R_{ab} defined in Eq. (34) are linear combinations of the $R_{ab}^{\alpha\beta}$

$$R_{ab}=(R_{ab}^{++}+R_{ab}^{--})+(R_{ab}^{+-}+R_{ab}^{-+})\ . \tag{61}$$

It is now easy to see that the observables given in Table III fall into two classes, depending on how $\tilde{\rho}_N^{\pm}$ are paired with $\tilde{\rho}_D^{\pm}$. Amplitudes in class I are those observables which occur as the following linear combinations:

$$R_{ab}+(-1)^{a+b}R_{-a-b}=2(R_{ab}^{++}+R_{ab}^{--})\ . \tag{62a}$$

These are R_L, R_T, $R_{TT}^{(\mathrm{I})}$, $R_{LT}^{(\mathrm{I})}$, and $R_{LT'}^{(\mathrm{I})}$. (This is the origin of the superscript I.) Those in class II are the following:

$$R_{ab}-(-1)^{a+b}R_{-a-b}=2(R_{ab}^{+-}+R_{ab}^{-+}) \tag{62b}$$

and are $R_{T'}$ and the three interference terms with the superscript (II). The amplitudes which are members of each class are listed in Table V, and the nonzero observables are identified in Table VI. If an observable is in class I, then all entries labeled II in Table VI are zero for that observable. In particular, since the cross section for unpolarized hadrons arises from a $\tilde{\rho}_N^{+}\tilde{\rho}_D^{+}$ pairing, only amplitudes in class I can contribute, and the familiar result that the cross section depends on only five structure functions is obtained.

Before we present explicit formulas for the observables, it is convenient to make further simplifications by introducing hybrid amplitudes.

E. Polarization observables in a hybrid basis

The density matrices given in Eqs. (57) and (58) are even or odd under the Y parity transformation, but still have the complexity (number of nonzero elements) of the original density matrices. The reason for this is that these matrices are expressed in terms of the helicity basis, where the axis of quantization is along z, the direction of motion. However, since only the y component of spin does not change sign under the Y transformation (none of the components of spin change under parity, but the rotation by π around the y axis changes $x\rightarrow -x$ and $z\rightarrow -z$) it is more natural to choose the y axis attached to the particle as the basis for quantization. Amplitudes quantized with respect to the y axis are referred to as transversity amplitudes. The amplitudes introduced here quantize all the hadrons with respect to the y axis, but do not treat the photon in this fashion. For this reason, they will be called *hybrid* amplitudes. They are linear combinations of helicity amplitudes which greatly simplify the final results.[4]

The density matrices (57), expressed in this hybrid basis, have the components P_z and P_z' occupying the locations of P_y and P_y', while P_y and P_y' are mapped into $-P_z$ and $-P_z'$ along the diagonal. Formally, this is accomplished by a rotation by $-\pi/2$ about the x axis, which carries $P_z\rightarrow P_y$ and $P_y\rightarrow -P_z$, leaving P_x unchanged.[12] The new density matrices, which will be distinguished from (57) and (58) by discarding the tilde, are

TABLE V. The two classes of observables which occur in electrodisintegration. This separation is a consequence of Y parity conservation.

Class I $\tilde{\rho}_N^{+}\tilde{\rho}_D^{+}$ or $\tilde{\rho}_N^{-}\tilde{\rho}_D^{-}$	Class II $\tilde{\rho}_N^{+}\tilde{\rho}_D^{-}$ or $\tilde{\rho}_N^{-}\tilde{\rho}_D^{+}$
R_L	
R_T	$R_{T'}$
$R_{TT}^{(\mathrm{I})}$	$R_{TT}^{(\mathrm{II})}$
$R_{LT}^{(\mathrm{I})}$	$R_{LT}^{(\mathrm{II})}$
$R_{LT'}^{(\mathrm{I})}$	$R_{LT'}^{(\mathrm{II})}$

TABLE VI. The nonzero observables in each class. If the entry I occurs, this observable is zero for observables of Class II, and conversely.

	U	$\tilde{T}_{10}$	$\tilde{T}_{20}$	$\mathrm{Im}\tilde{T}_{11}$	$\mathrm{Re}\tilde{T}_{11}$	$\mathrm{Im}\tilde{T}_{21}$	$\mathrm{Re}\tilde{T}_{21}$	$\mathrm{Im}\tilde{T}_{22}$	$\mathrm{Re}\tilde{T}_{22}$
U	I	II	I	I	II	II	I	II	I
P_x	II	I	II	II	I	I	II	I	II
P_y	I	II	I	I	II	II	I	II	I
P_z	II	I	II	II	I	I	II	I	II

$$\rho_N^+=\frac{1}{4}\begin{bmatrix}1-P_y-P_y' & & & \\ & 1-P_y+P_y' & & \\ & & 1+P_y-P_y' & \\ & & & 1+P_y+P_y'\end{bmatrix},$$

$$\rho_N^-=\frac{1}{4}\begin{bmatrix}0 & P_x'-iP_z' & P_x-iP_z & 0\\ P_x'+iP_z' & 0 & 0 & P_x-iP_z\\ P_x+iP_z & 0 & 0 & P_x'-iP_z'\\ 0 & P_x+iP_z & P_x'+iP_z' & 0\end{bmatrix} \tag{63}$$

and

$$\rho_D^+=\frac{1}{3}\begin{bmatrix}1+\frac{1}{\sqrt{2}}T_{20}+\sqrt{\frac{3}{2}}T_{10} & 0 & \sqrt{3}T_{22}^*\\ 0 & 1-\sqrt{2}T_{20} & 0\\ \sqrt{3}T_{22} & 0 & 1+\frac{1}{\sqrt{2}}T_{20}-\sqrt{\frac{3}{2}}T_{10}\end{bmatrix},$$

$$\rho_D^-=\frac{-1}{3}\left[\frac{3}{2}\right]^{1/2}\begin{bmatrix}0 & (T_{11}^*+T_{21}^*) & 0\\ (T_{11}+T_{21}) & 0 & (T_{11}^*-T_{21}^*)\\ 0 & (T_{11}-T_{21}) & 0\end{bmatrix}, \tag{64}$$

where the T_{JM} are obtained from $\tilde{T}_{JM}$ by the substitution $z\to y$ and $y\to -z$ (see Table VII). The transformations which achieve these simplifications are

$$R_x^4(-\pi/2)=\frac{1}{2}\begin{bmatrix}1+i\sigma_x & \vdots & i-\sigma_x\\ \cdots & \cdots & \cdots\\ i-\sigma_x & \vdots & 1+i\sigma_x\end{bmatrix},$$

$$R_x^3(-\pi/2)=\frac{1}{2}\begin{bmatrix}1 & i\sqrt{2} & -1\\ i\sqrt{2} & 0 & i\sqrt{2}\\ -1 & i\sqrt{2} & 1\end{bmatrix}. \tag{65}$$

The hybrid amplitudes are related to the helicity amplitudes by

$$R_x^4(-\pi/2)\tilde{J}_+R_x^3(-\pi/2)^\dagger=\begin{bmatrix}g_8 & g_3 & g_{12}\\ g_1 & g_{10} & g_5\\ g_2 & g_9 & g_6\\ g_7 & g_4 & g_{11}\end{bmatrix}=J_+ \tag{66}$$

and

$$R_x^4(-\pi/2)\tilde{J}_0R_x^3(-\pi/2)^\dagger=\begin{bmatrix}0 & g_{15} & 0\\ g_{13} & 0 & g_{17}\\ g_{14} & 0 & g_{18}\\ 0 & g_{16} & 0\end{bmatrix}=J_0\ . \tag{67}$$

The specific linear combinations which define the g's are

TABLE VII. The deuteron tensor polarization densities in the hybrid basis. The subscripts x,y,z refer to the (x',y',z') coordinate system shown in Fig. 2.

$$T_{00}=1$$

$$T_{11}=-\frac{\sqrt{3}}{2}(P_x-iP_z)$$

$$T_{10}=\sqrt{\tfrac{3}{2}}P_y$$

$$T_{22}=\frac{1}{2\sqrt{3}}(P_{xx}-P_{zz}-2iP_{xz})$$

$$T_{21}=-\frac{1}{\sqrt{3}}(P_{xy}-iP_{zy})$$

$$T_{20}=\frac{1}{\sqrt{2}}P_{yy}$$

given in the Appendix.

The Y parity transformations take on a very simple form in this hybrid basis. They become

$$Y_4 = R_x^4(-\pi/2)\tilde{Y}_4 R_x^4(-\pi/2)^\dagger = \begin{bmatrix} 1 & & & \\ & -1 & & \\ & & -1 & \\ & & & 1 \end{bmatrix},$$
$$Y_3 = R_x^3(-\pi/2)\tilde{Y}_3 R_x^3(-\pi/2)^\dagger = \begin{bmatrix} -1 & & \\ & 1 & \\ & & -1 \end{bmatrix}. \tag{68}$$

The simplicity of the J_0 component of the current, Eq. (67) above, follows directly from the parity transformation, and the J_- current is obtained from Eq. (53), which also takes on a simple form:

$$Y_4 J_+ Y_3 = -J_- = \begin{bmatrix} -g_8 & g_3 & -g_{12} \\ g_1 & -g_{10} & g_5 \\ g_2 & -g_9 & g_6 \\ -g_7 & g_4 & -g_{11} \end{bmatrix}. \tag{69}$$

This relation suggests separation of the $J_\pm$ currents into pieces even or odd under the Y transformation

$$J_s = \tfrac{1}{2}(J_+ - J_-) = \begin{bmatrix} 0 & g_3 & 0 \\ g_1 & 0 & g_5 \\ g_2 & 0 & g_6 \\ 0 & g_4 & 0 \end{bmatrix},$$
$$J_a = \tfrac{1}{2}(J_+ + J_-) = \begin{bmatrix} g_8 & 0 & g_{12} \\ 0 & g_{10} & 0 \\ 0 & g_9 & 0 \\ g_7 & 0 & g_{11} \end{bmatrix}. \tag{70}$$

The structure functions of Table III, when expressed in terms of these amplitudes, take on a beautifully simple and symmetric form, given in Table VIII.

Examination of Table VIII shows that the nine structure functions divide into three groups of 2, each of which give the real and imaginary parts of sums over products of two different currents, and three functions related to squares of each of the currents. Table IX shows the patterns in a symbolic way.

It is also possible to reduce all the sums to only one generic sum, which we take to be $\sum_{\rm I} J_0 J_s$. The specific results for the two observables which depend on this sum are presented in Table X as real and imaginary parts of sums over the bilinear products $g_i^* g_{i+12}$ where i runs from 1 to 6. The results for the moduli $|J_0|^2$ and $|J_s|^2$ can be obtained from this sum by substituting for $g_i^* g_{i+12}$ the combinations $|g_i|^2$ and $|g_{i+12}|^2$, as shown in Table XI. The observables involving $|J_a|^2$ can be obtained by observing that the 4×4 matrix, which can be written in 2×2 block form

$$S = \begin{bmatrix} 0 & 1 \\ 1 & 0 \end{bmatrix}, \tag{71}$$

maps J_a into a symmetric form with $g_i \to g_{i+6}$

$$SJ_a = \begin{bmatrix} 0 & g_9 & 0 \\ g_7 & 0 & g_{11} \\ g_8 & 0 & g_{12} \\ 0 & g_{10} & 0 \end{bmatrix}. \tag{72}$$

However, S changes the sign of P_y and P_z in the proton density matrices as follows:

$$S\rho_N^+ S = \begin{bmatrix} 1+P_y & 0 \\ 0 & 1-P_y \end{bmatrix},$$
$$S\rho_N^- S = \begin{bmatrix} 0 & P_x + iP_z \\ P_x - iP_z & 0 \end{bmatrix}. \tag{73}$$

Hence $\sum |J_a|^2$ can be obtained from $\sum |J_s|^2$ by substituting $|g_{i+6}|^2$ for $|g_i|^2$ and *changing the sign of P_y and P_z*. This substitution and extra phase (ϵ) is indicated in Table XI. Finally, the four sums of type II involving a product of a symmetric and an antisymmetric current can be handled by using (72) and noting that a single S operating on the proton polarization density matrix converts the forms of $\rho_N^\pm$ into each other:

TABLE VIII. The nine structure functions which enter the cross section given in terms of the longitudinal, the symmetric (J_s), and the antisymmetric (J_a) current operators defined in Eq. (70). These results can be obtained by inspection from the second column of Table III and from Table V.

$$R_L = \eta^2 \sum_{\rm I} |J_0|^2$$
$$R_T = 2\sum_{\rm I} \{|J_s|^2 + |J_a|^2\} \qquad R_{LT}^{(\rm I)} = 4\eta\,\mathrm{Re}\sum_{\rm I} J_0 J_s^\dagger$$
$$R_{TT}^{(\rm I)} = 2\sum_{\rm I} \{|J_a|^2 - |J_s|^2\} \qquad R_{LT'}^{(\rm I)} = 4\eta\,\mathrm{Im}\sum_{\rm I} J_0 J_s^\dagger$$
$$R_{TT}^{(\rm II)} = -4\,\mathrm{Im}\sum_{\rm II} J_s J_a^\dagger \qquad R_{LT'}^{(\rm II)} = 4\eta\,\mathrm{Re}\sum_{\rm II} J_0 J_a^\dagger$$
$$R_{T'} = 4\,\mathrm{Re}\sum_{\rm II} J_s J_a^\dagger \qquad R_{LT}^{(\rm II)} = 4\eta\,\mathrm{Im}\sum_{\rm II} J_0 J_a^\dagger$$
$$\text{where } \sum_{\rm I} J_a J_b^\dagger = 4\kappa^2 \mathrm{tr}\{\rho_N^+ J_a \rho_D^+ J_b^\dagger + \rho_N^- J_a \rho_D^- J_b^\dagger\}$$
$$\sum_{\rm II} J_a J_b^\dagger = 4\kappa^2 \mathrm{tr}\{\rho_N^+ J_a \rho_D^- J_b^\dagger + \rho_N^- J_a \rho_D^+ J_b^\dagger\}$$

TABLE IX. Symbolic representation of the content of the nine observables given in Table VIII. The ith diagonal element of the array is proportional to the square of the modulus of the ith current component $|J_i|^2$, and the (i,j) elements are proportional to the products $J_i J_j^\dagger$. If the element is to the upper right of the diagonal it is proportional to $\mathrm{Re}(J_i J_j^\dagger)$; elements to the lower left of the diagonal are proportional to $\mathrm{Im}(J_i J_j^\dagger)$.

	J_0	J_s	J_a
J_0	R_L	$R_{LT}^{(\rm I)}$	$R_{LT'}^{(\rm II)}$
J_s	$R_{LT'}^{(\rm I)}$	$R_T - R_{TT}^{(\rm I)}$	$R_{T'}$
J_a	$R_{LT}^{(\rm II)}$	$R_{TT}^{(\rm II)}$	$R_T + R_{TT}^{(\rm I)}$

$$S\rho_N^- = \begin{bmatrix} P_x + iP_z & 0 \\ 0 & P_x - iP_z \end{bmatrix}, \qquad S\rho_N^+ = \begin{bmatrix} 0 & 1+P_y \\ 1-P_y & 0 \end{bmatrix}. \tag{74}$$

Hence the sums of type II have the same general structure as those of type I but with $(1, P_y, P_x, iP_z) \rightarrow (P_x, -iP_z, 1, -P_y)$. These observables are given in Table XII. The structure of the results are different because of the transformations (74), but can be expressed in terms of the same sets of amplitudes (the $a-f$ defined in Table X) with the substitutions indicated.

Finally, the neutron observables can be obtained from

TABLE X. The observables which depend on the sum $\sum_{\mathrm{I}} J_0 J_s$. The quantity $A(P_j, T_i)$ is given in the table; only proton polarizations are considered here, and $z''=l$, $y''=n$, $x''=s$. To construct the observable it is necessary to multiply the result by the factor shown at the top of each block; for example, $R_{LT}(P_n, T_{20}) = \frac{4}{3}\eta\kappa^2 \mathrm{Re}(a_3 - b_3)$. In order to determine any given product, for example, $g_1^* g_{13}$, it is necessary to measure the set of all quantities which contain this product, the three b_i's, for example. The quantities break naturally into different disjoint sets which are labeled with the same lower case letter $a,b,c,d,e,f,$. The reader can easily find the patterns after a short study.

	U	P_n	P_s	P_l
	$R_{LT}^{(\mathrm{I})}$:	$R_{LT}(P_j, T_i) = \frac{4}{3}\eta\kappa^2 A(P_j, T_i)$		
U	$\mathrm{Re}(a_1 + b_1)$	$\mathrm{Re}(a_1 - b_1)$		
$\sqrt{\frac{3}{2}} T_{10}$	$\mathrm{Re}(a_2 + b_2)$	$\mathrm{Re}(a_2 - b_2)$		
$\frac{1}{\sqrt{2}} T_{20}$	$\mathrm{Re}(a_3 + b_3)$	$\mathrm{Re}(a_3 - b_3)$		
$\sqrt{3}\mathrm{Re}T_{22}$	$\mathrm{Re}(c_1 + d_1)$	$\mathrm{Re}(c_1 - d_1)$		
$\sqrt{3}\mathrm{Im}T_{22}$	$-\mathrm{Im}(c_2 + d_2)$	$-\mathrm{Im}(c_2 - d_2)$		
$\sqrt{\frac{3}{2}}\mathrm{Re}T_{11}$			$-\mathrm{Re}(e_1 + f_1)$	$-\mathrm{Im}(e_1 - f_1)$
$\sqrt{\frac{3}{2}}\mathrm{Im}T_{11}$			$\mathrm{Im}(e_2 + f_2)$	$-\mathrm{Re}(e_2 - f_2)$
$\sqrt{\frac{3}{2}}\mathrm{Re}T_{21}$			$-\mathrm{Re}(e_3 + f_3)$	$-\mathrm{Im}(e_3 - f_3)$
$\sqrt{\frac{3}{2}}\mathrm{Im}T_{21}$			$\mathrm{Im}(e_4 + f_4)$	$-\mathrm{Re}(e_4 - f_4)$
	$R_{LT'}^{(\mathrm{I})}$:	$R_{LT'}(P_j, T_i) = \frac{4}{3}\eta\kappa^2 A(P_j, T_i)$		
U	$\mathrm{Im}(a_1 + b_1)$	$\mathrm{Im}(a_1 - b_1)$		
$\sqrt{\frac{3}{2}} T_{10}$	$\mathrm{Im}(a_2 + b_2)$	$\mathrm{Im}(a_2 - b_2)$		
$\frac{1}{\sqrt{2}} T_{20}$	$\mathrm{Im}(a_3 + b_3)$	$\mathrm{Im}(a_3 - b_3)$		
$\sqrt{3}\mathrm{Re}T_{22}$	$\mathrm{Im}(c_1 + d_1)$	$\mathrm{Im}(c_1 - d_1)$		
$\sqrt{3}\mathrm{Im}T_{22}$	$\mathrm{Re}(c_2 + d_2)$	$\mathrm{Re}(c_2 - d_2)$		
$\sqrt{\frac{3}{2}}\mathrm{Re}T_{11}$			$-\mathrm{Im}(e_1 + f_1)$	$\mathrm{Re}(e_1 - f_1)$
$\sqrt{\frac{3}{2}}\mathrm{Im}T_{11}$			$-\mathrm{Re}(e_2 + f_2)$	$-\mathrm{Im}(e_2 - f_2)$
$\sqrt{\frac{3}{2}}\mathrm{Re}T_{21}$			$-\mathrm{Im}(e_3 + f_3)$	$\mathrm{Re}(e_3 - f_3)$
$\sqrt{\frac{3}{2}}\mathrm{Im}T_{21}$			$-\mathrm{Re}(e_4 + f_4)$	$-\mathrm{Im}(e_4 - f_4)$

$a_1 = g_2^* g_{14} + g_4^* g_{16} + g_6^* g_{18}$
$a_2 = g_2^* g_{14} - g_6^* g_{18}$
$a_3 = g_2^* g_{14} - 2g_4^* g_{16} + g_6^* g_{18}$

$b_1 = g_1^* g_{13} + g_3^* g_{15} + g_5^* g_{17}$
$b_2 = g_1^* g_{13} - g_5^* g_{17}$
$b_3 = g_1^* g_{13} - 2g_3^* g_{15} + g_5^* g_{17}$

$c_1 = g_2^* g_{18} + g_6^* g_{14}$
$c_2 = g_2^* g_{18} - g_6^* g_{14}$

$d_1 = g_1^* g_{17} + g_5^* g_{13}$
$d_2 = g_1^* g_{17} - g_5^* g_{13}$

$e_1 = (g_1 + g_5)^* g_{16} + g_3^* (g_{18} + g_{14})$
$e_2 = (g_1 - g_5)^* g_{16} + g_3^* (g_{18} - g_{14})$
$e_3 = (g_1 - g_5)^* g_{16} - g_3^* (g_{18} - g_{14})$
$e_4 = (g_1 + g_5)^* g_{16} - g_3^* (g_{18} + g_{14})$

$f_1 = (g_2 + g_6)^* g_{15} + g_4^* (g_{17} + g_{13})$
$f_2 = (g_2 - g_6)^* g_{15} + g_4^* (g_{17} - g_{13})$
$f_3 = (g_2 - g_6)^* g_{15} - g_4^* (g_{17} - g_{13}),$
$f_4 = (g_2 + g_6)^* g_{15} - g_4^* (g_{17} + g_{13})$

TABLE XI. The observables which depend on $\Sigma|J_0|^2$, $\Sigma|J_s|^2$, and $\Sigma|J_a|^2$. Again the quantity $A(P_j,T_i)$ is given in the table. Sets of quantities which depend on moduli $|g_i|^2$ are denoted by capitalized *italic* letters. Otherwise, the notation is as in Table X. For the observables $R_T+R_{TT}^{(\mathrm{I})}$, the relations are $R_T^+(P_j,T_i)=\frac{4}{3}\kappa^2 A(P_j,T_i)$ with all $g_i\to g_{i+6}$ and the phase $\epsilon=-1$. For R_L, the relations are $R_L(P_j,T_i)=\eta^2\kappa^2 A(P_j,T_i)$ with all $g_i\to g_{i+12}$ and $\epsilon=1$.

	U	P_n	P_s	P_l
	$R_T-R_{TT}^{(\mathrm{I})}$:	$R_T^-(P_j,T_i)=\frac{4}{3}\kappa^2 A(P_j,T_i)$, $\epsilon=1$		
U	A_1+B_1	$\epsilon(A_1-B_1)$		
$\sqrt{\frac{3}{2}}T_{10}$	A_2+B_2	$\epsilon(A_2-B_2)$		
$\frac{1}{\sqrt{2}}T_{20}$	A_3+B_3	$\epsilon(A_3-B_3)$		
$\sqrt{3}\mathrm{Re}T_{22}$	$\mathrm{Re}(c+d)$	$\epsilon\mathrm{Re}(c-d)$		
$\sqrt{3}\mathrm{Im}T_{22}$	$-\mathrm{Im}(c+d)$	$-\epsilon\mathrm{Im}(c-d)$		
$\sqrt{\frac{3}{2}}\mathrm{Re}T_{11}$			$-\mathrm{Re}(\alpha_1+\beta_1)$	$-\epsilon\mathrm{Im}(\alpha_1+\beta_1)$
$\sqrt{\frac{3}{2}}\mathrm{Im}T_{11}$			$\mathrm{Im}(\alpha_1-\beta_1)$	$-\epsilon\mathrm{Re}(\alpha_1-\beta_1)$
$\sqrt{\frac{3}{2}}\mathrm{Re}T_{21}$			$-\mathrm{Re}(\alpha_2+\beta_2)$	$-\epsilon\mathrm{Im}(\alpha_2+\beta_2)$
$\sqrt{\frac{3}{2}}\mathrm{Im}T_{21}$			$\mathrm{Im}(\alpha_2-\beta_2)$	$-\epsilon\mathrm{Re}(\alpha_2-\beta_2)$
$A_1=\lvert g_2\rvert^2+\lvert g_4\rvert^2+\lvert g_6\rvert^2$		$B_1=\lvert g_1\rvert^2+\lvert g_3\rvert^2+\lvert g_5\rvert^2$		$\alpha_1=2g_1^*g_4+2g_3^*g_6$
$A_2=\lvert g_2\rvert^2-\lvert g_6\rvert^2$		$B_2=\lvert g_1\rvert^2-\lvert g_5\rvert^2$		$\alpha_2=2g_1^*g_4-2g_3^*g_6$
$A_3=\lvert g_2\rvert^2-2\lvert g_4\rvert^2+\lvert g_6\rvert^2$		$B_3=\lvert g_1\rvert^2-2\lvert g_3\rvert^2+\lvert g_5\rvert^2$		
				$\beta_1=2g_3^*g_2+2g_5^*g_4$
$c=2g_2^*g_6$		$d=2g_1^*g_5$		$\beta_2=2g_3^*g_2-2g_5^*g_4$

TABLE XII. The observables of type II. The notation is the same as in Table X. For $R_{T'}$ and $R_{TT}^{(\mathrm{II})}$ use the $a's-f's$ of Table X with $g_{i+12}\to g_i$, $g_i^*\to g_{i+6}^*$. For $R_{LT'}^{(\mathrm{II})}$ and $R_{LT}^{(\mathrm{II})}$ use the $a's-f's$ of Table X with g_{i+12} unchanged, $g_i^*\to g_{i+6}^*$.

	U	P_n	P_s	P_l
		$R_{LT'}^{(\mathrm{II})}$: $R_{LT'}(P_j,T_i)=4\eta\kappa^2 A(P_j,T_i)$		
		$R_{T'}$: $R_{T'}(P_j,T_i)=4\kappa^2 A(P_j,T_i)$		
U			$\mathrm{Re}(a_1+b_1)$	$\mathrm{Im}(a_1-b_1)$
$\sqrt{\frac{3}{2}}T_{10}$			$\mathrm{Re}(a_2+b_2)$	$\mathrm{Im}(a_2-b_2)$
$\frac{1}{\sqrt{2}}T_{20}$			$\mathrm{Re}(a_3+b_3)$	$\mathrm{Im}(a_3-b_3)$
$\sqrt{3}\mathrm{Re}T_{22}$			$\mathrm{Re}(c_1+d_1)$	$\mathrm{Im}(c_1-d_1)$
$\sqrt{3}\mathrm{Im}T_{22}$			$-\mathrm{Im}(c_2+d_2)$	$\mathrm{Re}(c_2-d_2)$
$\sqrt{\frac{3}{2}}\mathrm{Re}T_{11}$	$-\mathrm{Re}(e_1+f_1)$	$-\mathrm{Re}(e_1-f_1)$		
$\sqrt{\frac{3}{2}}\mathrm{Im}T_{11}$	$\mathrm{Im}(e_2+f_2)$	$\mathrm{Im}(e_2-f_2)$		
$\sqrt{\frac{3}{2}}\mathrm{Re}T_{21}$	$-\mathrm{Re}(e_3+f_3)$	$-\mathrm{Re}(e_3-f_3)$		
$\sqrt{\frac{3}{2}}\mathrm{Im}T_{21}$	$\mathrm{Im}(e_4+f_4)$	$\mathrm{Im}(e_4-f_4)$		
		$R_{LT}^{(\mathrm{II})}$: $R_{LT}(P_j,T_i)=4\eta\kappa^2 A(P_j,T_i)$		
		$R_{TT}^{(\mathrm{II})}$: $R_{TT}(P_j,T_i)=-4\kappa^2 A(P_j,T_i)$		
U			$\mathrm{Im}(a_1+b_1)$	$-\mathrm{Re}(a_1-b_1)$
$\sqrt{\frac{3}{2}}T_{10}$			$\mathrm{Im}(a_2+b_2)$	$-\mathrm{Re}(a_2-b_2)$
$\frac{1}{\sqrt{2}}T_{20}$			$\mathrm{Im}(a_3+b_3)$	$-\mathrm{Re}(a_3-b_3)$
$\sqrt{3}\mathrm{Re}T_{22}$			$\mathrm{Im}(c_1+d_1)$	$-\mathrm{Re}(c_1-d_1)$
$\sqrt{3}\mathrm{Im}T_{22}$			$\mathrm{Re}(c_2+d_2)$	$\mathrm{Im}(c_2-d_2)$
$\sqrt{\frac{3}{2}}\mathrm{Re}T_{11}$	$-\mathrm{Im}(e_1+f_1)$	$-\mathrm{Im}(e_1-f_1)$		
$\sqrt{\frac{3}{2}}\mathrm{Im}T_{11}$	$-\mathrm{Re}(e_2+f_2)$	$-\mathrm{Re}(e_2-f_2)$		
$\sqrt{\frac{3}{2}}\mathrm{Re}T_{21}$	$-\mathrm{Im}(e_3+f_3)$	$-\mathrm{Im}(e_3-f_3)$		
$\sqrt{\frac{3}{2}}\mathrm{Im}T_{21}$	$-\mathrm{Re}(e_4+f_4)$	$-\mathrm{Re}(e_4-f_4)$		

the proton observables by noting that the matrix B

$$B=\begin{bmatrix}1&0&0&0\\0&0&1&0\\0&1&0&0\\0&0&0&1\end{bmatrix} \tag{75}$$

transforms neutron density matrices into proton-like density matrices

$$B\begin{bmatrix}1-\sigma_z P'_y & \\ & 1-\sigma_z P'_y\end{bmatrix}B=\begin{bmatrix}1-P'_y & \\ & 1+P'_y\end{bmatrix}, \tag{76}$$

$$B\begin{bmatrix}\sigma_x P'_x+\sigma_y P'_z & 0\\ 0 & \sigma_x P'_x+\sigma_y P'_z\end{bmatrix}B=\begin{bmatrix}0 & P'_x-iP'_z\\ P'_x+iP'_z & 0\end{bmatrix},$$

while its only effect on the symmetric current is to interchange $g_1\leftrightarrow g_2$ and $g_5\leftrightarrow g_6$:

$$B\begin{bmatrix}0&g_3&0\\g_1&0&g_5\\g_2&0&g_6\\0&g_4&0\end{bmatrix}=\begin{bmatrix}0&g_3&0\\g_2&0&g_6\\g_1&0&g_5\\0&g_4&0\end{bmatrix} \tag{77}$$

and on the antisymmetric current it interchanges $g_9\leftrightarrow g_{10}$:

$$B\begin{bmatrix}g_8&0&g_{12}\\0&g_{10}&0\\0&g_9&0\\g_7&0&g_{11}\end{bmatrix}=\begin{bmatrix}g_8&0&g_{12}\\0&g_9&0\\0&g_{10}&0\\g_7&0&g_{11}\end{bmatrix}. \tag{78}$$

Hence, all neutron observables have a structure identical to the corresponding proton observable except that for J_s we must interchange $g_1\leftrightarrow g_2$ and $g_5\leftrightarrow g_6$, for J_a we interchange $g_9\leftrightarrow g_{10}$, and for J_0 we interchange $g_{13}\leftrightarrow g_{14}$ and $g_{17}\leftrightarrow g_{18}$.

The calculation of the 18 observables which go with each of the nine structure functions can now be done by hand. The results have been presented in Tables X–XII. [These results were also confirmed using the symbolic manipulation program (SMP).] The patterns outlined above can be readily seen in the final results. These tables, together with Eq. (30) for the cross section, are the principal results of this paper.

It may sometimes be necessary to identify a particular observable in the tables. The structure functions will be labeled and identified by the following expansion, given for the pair $R_{LT}^{(\mathrm{I})}$ and $R_{LT}^{(\mathrm{II})}$ as an example:

$$\begin{aligned}R_{LT}^{(\mathrm{I})}&=\sum_{i,j\in \mathrm{I}} T_i P_j R_{LT}(P_j,T_i)\ ,\\ R_{LT}^{(\mathrm{II})}&=\sum_{i,j\in \mathrm{II}} T_i P_j R_{LT}(P_j,T_i)\ ,\end{aligned} \tag{79}$$

where

$$T_i=\left\{U,\sqrt{\tfrac{3}{2}}T_{10},\frac{1}{\sqrt{2}}T_{20},\sqrt{3}\,\mathrm{Re}T_{22},\sqrt{3}\,\mathrm{Im}T_{22},\sqrt{\tfrac{3}{2}}\mathrm{Re}T_{11},\sqrt{\tfrac{3}{2}}\mathrm{Im}T_{11},\sqrt{\tfrac{3}{2}}\mathrm{Re}T_{21},\sqrt{\tfrac{3}{2}}\mathrm{Im}T_{21}\right\}, \tag{80}$$
$$P_j=\{U,P_n,P_s,P_l\}\ ,$$

and the nonzero terms in each sum for hybrid amplitudes are given in Tables X–XII. In identifying specific terms, we will suppress the U labels, and adopt other simplifying notation as illustrated below:

$$\begin{aligned}&R_{LT}(U,U)=R_{LT}\ ,\\ &R_{LT}(P_n,U)=R_{LT}(n)\ ,\\ &R_{LT}(U,\sqrt{3}\mathrm{Im}T_{22})=R_{LT}(\mathrm{Im}T_{22})\ ,\\ &R_{LT}(P_n,\sqrt{3}\mathrm{Im}T_{22})=R_{LT}(n,\mathrm{Im}T_{22})\ .\end{aligned} \tag{81}$$

Note that, because classes I and II are disjoint, the subscripts on $R_{LT}^{(\mathrm{I,II})}$ have been suppressed in the expansions (79); the arguments of $R_{LT}(P_j,T_i)$ uniquely identify to which expansion it belongs. This notation forces a pairing of $R_{LT}^{(\mathrm{I})}$ and $R_{LT}^{(\mathrm{II})}$, but as shown in Tables VII, IX, and X–XII, the natural pairing is between $R_{LT}^{(\mathrm{I})}$ and $R_{LT'}^{(\mathrm{I})}$, for example. For the special case of the amplitudes $R_T\pm R_{TT}^{(\mathrm{I})}$ we will sometimes use the notation $R_T^{\pm}$ for the expansion coefficients in Eq. (79).

F. Photodisintegration cross section

The differential cross section for photodisintegration can be obtained quickly from our previous work. The most general polarization state of a real photon can be written as a linear combination of its two helicity states,

$$\epsilon^\mu=a\epsilon_+^\mu+b\epsilon_-^\mu \tag{82}$$

where $|a|^2+|b|^2=1$. Then the differential cross section in the c.m. system is

$$d\sigma_\gamma=\frac{e^2}{4\nu_0 W}\rho^\gamma_{\lambda\lambda'}W_{\lambda\lambda'}\ , \tag{83}$$

where the hadron density was defined in Eq. (11), ν_0 is the c.m. energy of the photon (note that $\nu_0=q_0$), and the photon density matrix is

$$\rho^\gamma_{\lambda\lambda'}=\begin{bmatrix}|a|^2 & ab^*\\ ba^* & |b|^2\end{bmatrix}. \tag{84}$$

Using the hermiticity of $W_{\lambda\lambda'}$, and reducing in the c.m. as done in Eq. (26), gives immediately

$$\frac{d\sigma}{d\Omega_1}=e^2\left[\frac{p_1}{8\nu_0 W}\right][R_T+(|a|^2-|b|^2)R_{T'} +2\,\mathrm{Re}(ab^*)R_{TT}^{(\mathrm{I})} +2\,\mathrm{Im}(ab^*)R_{TT}^{(\mathrm{II})}] , \tag{85}$$

where the R's are the same structure functions discussed in the preceding sections, except that they are evaluated at the real photon point $q^2=0$.

G. Inclusive cross sections

Inclusive electrodisintegration cross sections can be readily obtained by integrating over the solid angle $d\Omega_1$, and summing over all polarizations of the outgoing nucleons. We will present formulas with and without deuteron polarization.

Special care must be taken with the deuteron polarization. Recall that the results given in Tables X–XII were for deuteron polarizations defined in the *ejectile* plane, rotated through the angle ϕ with respect to the *electron* scattering plane. When integrating over ϕ to obtain inclusive cross sections, care must be taken to express the deuteron polarizations with respect to the electron scattering plane, which is fixed. To avoid any confusion, the polarizations defined with respect to the *electron* scattering plane will be denoted by $T_{ij}^{(0)}$ to distinguish them from T_{ij}, the polarizations defined in the ejectile plane.

To express the polarizations $T_{ij}^{(0)}$ in the ejectile plane, we must rotate the coordinate axes through angle ϕ about the z axis, which is equivalent to an active rotation of the polarization quantities $T_{ij}^{(0)}$ through angle $-\phi$. This is the same transformation we carried out on the virtual photon polarization vector in Sec. II B. However, we have chosen to define the deuteron T_{ij} with respect to the y axis, and this makes the transformation laws more complex than that obtained in Eq. (22) for the photon. The correct transformation laws are

$$\begin{aligned}
\mathrm{Re}T_{11}&=\cos\phi\,\mathrm{Re}T_{11}^{(0)}-\sin\phi\left[\frac{T_{10}^{(0)}}{\sqrt{2}}\right] ,\\
\frac{T_{10}}{\sqrt{2}}&=\sin\phi\,\mathrm{Re}T_{11}^{(0)}+\cos\phi\left[\frac{T_{10}^{(0)}}{\sqrt{2}}\right] ,\\
\mathrm{Im}T_{11}&=\mathrm{Im}T_{11}^{(0)} ,\\
\mathrm{Re}T_{22}+\frac{1}{\sqrt{6}}T_{20}&=\mathrm{Re}T_{22}^{(0)}+\frac{1}{\sqrt{6}}T_{20}^{(0)} ,\\
\mathrm{Re}T_{22}-\sqrt{\tfrac{3}{2}}T_{20}&=\cos2\phi(\mathrm{Re}T_{22}^{(0)}-\sqrt{\tfrac{3}{2}}T_{20}^{(0)})\\
&\quad-\sin2\phi(2\,\mathrm{Re}T_{21}^{(0)}) ,\\
2\,\mathrm{Re}T_{21}&=\sin2\phi(\mathrm{Re}T_{22}^{(0)}-\sqrt{\tfrac{3}{2}}T_{20}^{(0)})+\cos2\phi(2\,\mathrm{Re}T_{21}^{(0)}) ,\\
\mathrm{Im}T_{22}&=\cos\phi\,\mathrm{Im}T_{22}^{(0)}-\sin\phi\,\mathrm{Im}T_{21}^{(0)} ,\\
\mathrm{Im}T_{21}&=\sin\phi\,\mathrm{Im}T_{22}^{(0)}+\cos\phi\,\mathrm{Im}T_{21}^{(0)} .
\end{aligned} \tag{86}$$

These give the deuteron polarization parameters in the *ejectile* plane (those used in Tables X–XII) in terms of polarization parameters in the *electron* scattering plane. These transformations *must* be used when calculating inclusive cross sections, where the deuteron target polarization is *fixed* as we integrate over ϕ. For exclusive measurements the deuteron polarization could be oriented with respect to the ejectile plane, in which case the results in Tables X–XII could be used directly. However, if a number of ϕ angles are measured simultaneously with a fixed deuteron polarization, as would be the case with the STAR spectrometer proposed for use at CEBAF by the Illinois group,[13] it would also be necessary to use the transformations (86) in order to predict the correct ϕ dependence of the cross sections.

Using the transformations (86) is it straightforward to carry out the ϕ integrations analytically. The integrations over θ_1 cannot be carried out unless the structure functions are known; we will denote these integrations by

$$\bar{R}_A(T_B)=\frac{1}{2}\int_0^\pi \sin\theta_1 d\theta_1 R_A(T_B) . \tag{87}$$

Using this notation, the most general inclusive cross section can be obtained from Eq. (30). It becomes

$$\begin{aligned}
\frac{d^3\sigma}{d\Omega' dE'}=\sigma_M&\left[\left[\frac{W}{M_T}\right]^2 v_L[W_L+P_{zz}^{(0)}W_L(P_{zz})]+v_T[W_T+P_{zz}^{(0)}W_T(P_{zz})]+v_{TT}(P_{xx}^{(0)}-P_{yy}^{(0)})W_{TT}\right.\\
&+\left[\frac{W}{M_T}\right]v_{TL}[P_y^{(0)}W_{LT}(P_y)+P_{xz}^{(0)}W_{LT}(P_{xz})]+2hv_T'P_z^{(0)}W_{T'}\\
&\left.+2h\left[\frac{W}{M_T}\right]v_{TL}'[P_x^{(0)}W_{LT'}(P_x)+P_{yz}^{(0)}W_{LT'}(P_{yz})]\right] ,
\end{aligned} \tag{88}$$

where the deuteron polarizations $T_{JM}^{(0)}$ have been expressed in Cartesian form to facilitate interpretation of the results, and the inclusive structure functions W are given in terms of the $\bar{R}$'s of Eq. (87) by

$$W_L=\lambda\bar{R}_L \ ,$$

$$W_T=\lambda\bar{R}_T \ ,$$

$$W_L(P_{zz})=-\frac{\lambda}{4}[\bar{R}_L(T_{20})+3\bar{R}_L(\mathrm{Re}T_{22})] \ ,$$

$$W_{T'}(P_{zz})=-\frac{\lambda}{4}[\bar{R}_{T'}(T_{20})+3\bar{R}_{T'}(\mathrm{Re}T_{22})] \ ,$$

$$W_{TT}=\frac{\lambda}{8}[\bar{R}_{TT}(\mathrm{Re}T_{22})-\bar{R}_{TT}(T_{20})+\sqrt{2}\bar{R}_{TT}(ReT_{21})] \ , \tag{89}$$

$$W_{LT'}(P_y)=\frac{3\lambda}{4}\left[\bar{R}_{LT'}(T_{10})-\frac{1}{\sqrt{2}}\bar{R}_{LT'}(\mathrm{Re}T_{11})\right] \ ,$$

$$W_{LT'}(P_{xz})=-\frac{\lambda}{2}\left[\bar{R}_{LT'}(\mathrm{Im}T_{22})+\frac{1}{\sqrt{2}}\bar{R}_{LT'}(\mathrm{Im}T_{21})\right] \ ,$$

$$W_{T'}=\frac{3\lambda}{2\sqrt{2}}\bar{R}_{T'}(\mathrm{Im}T_{11}) \ ,$$

$$W_{LT'}(P_x)=\frac{-3\lambda}{4}\left[\bar{R}_{LT'}(T_{10})+\frac{1}{\sqrt{2}}\bar{R}_{LT'}(\mathrm{Re}T_{11})\right] \ ,$$

$$W_{LT'}(P_{yz})=-\frac{\lambda}{2}\left[\bar{R}_{LT'}(\mathrm{Im}T_{22})-\frac{1}{\sqrt{2}}\bar{R}_{LT'}(\mathrm{Im}T_{21})\right] \ ,$$

where $\lambda=p_1/M_T$. It has been known for some time[14] that time-reversal invariance implies that $W_{LT'}(P_y)=0$.

If the deuteron target is unpolarized, the cross section reduces to the familiar form

$$\frac{d^3\sigma}{d\Omega' dE'}=\sigma_M(W_2+2W_1\tan^2\theta/2) \ , \tag{90}$$

where

$$W_1=\tfrac{1}{2}W_T \ ,$$
$$W_2=\left[\frac{W}{M_T}\right]^2\frac{Q^4}{q_L^4}W_L+\frac{Q^2}{q_L^2}W_1 \ . \tag{91}$$

H. The cross sections and observables in lab frame

In the preceding sections, results for the hadronic currents were presented in the c.m. frame because of the convenience in obtaining inclusive cross sections. However, all observables are measured in the lab frame, so that it is necessary to completely clarify the relationship between these two frames.

A review of the derivations given in the preceding sections shows the following differences between the results presented so far (in which the electron variables are in the lab frame and the hadron variables are in the c.m. frame) and those in which all variables are in the lab frame.

(i) There is no boost operator Eq. (20). The primary effect of this is to remove the W/M_T factors from the J^0 components of the current, defined in Eq. (29).

(ii) The integration in Eq. (11) must be carried out in the lab frame. This introduces the recoil factor discussed below.

(iii) The polarization quantities must be transformed to the lab frame.

The effect of items (i) and (ii) is to introduce a recoil factor and a modified form for the cross section. The integration over the hadronic variables gives, in place of Eq. (26),

$$W'_{\lambda\lambda'}|_{\mathrm{lab}}=d\Omega_L p_L r R_{\lambda\lambda'} \ , \tag{92}$$

where

$$r=\frac{W}{M_T}\frac{1}{\left[1+\dfrac{\nu p_1-E_1 q\cos\theta_1}{M_T p_1}\right]_L} \ . \tag{93}$$

These changes give the following result for the cross section, Eq. (30), in the lab:

$$\frac{d^5\sigma}{d\Omega' dE' d\Omega_L}=\frac{\sigma_M p_L}{4\pi M_T}r\{v_L R_L+v_T R_T+v_{TT}[\cos2\phi R_{TT}^{(\mathrm{I})}+\sin2\phi R_{TT}^{(\mathrm{II})}]+v_{LT}[\cos\phi R_{LT}^{(\mathrm{I})}+\sin\phi R_{LT}^{(\mathrm{II})}]$$
$$+2hv'_T R_{T'}+2hv'_{LT}[\cos\phi R_{LT'}^{(\mathrm{II})}+\sin\phi R_{LT'}^{(\mathrm{I})}]\} \ , \tag{94}$$

where the structure functions R are to be evaluated in the lab frame with $\eta=q_L/Q$. Alternatively, if we work *only* with the covariant form of the longitudinal current, $J\cdot\epsilon_0$, the cross section can be written in the following alternative form:

$$\frac{d^5\sigma}{d\Omega' dE' d\Sigma}=\frac{\sigma_M}{4\pi M_T}\frac{Q^2}{q_L^2}\{\tilde{R}_L+s_T\tilde{R}_T-\tfrac{1}{2}[\cos2\phi\tilde{R}_{TT}^{(\mathrm{I})}+\sin2\phi\tilde{R}_{TT}^{(\mathrm{II})}]+s_{LT}[\cos\phi\tilde{R}_{LT}^{(\mathrm{I})}+\sin\phi\tilde{R}_{LT}^{(\mathrm{II})}]$$
$$+2hs'_T\tilde{R}_{T'}+2hs'_{LT}[\cos\phi\tilde{R}_{LT'}^{(\mathrm{II})}+\sin\phi\tilde{R}_{LT'}^{(\mathrm{I})}]\} \ , \tag{95}$$

where the $\tilde{R}$'s in Eq. (95) are now covariant, and are obtained from the covariant $R_{\lambda\lambda'}$ of Eq. (27) by setting $\eta=1$ in the *middle* column of Table III, and the s_i are

$$\begin{aligned} s_T &= \tfrac{1}{2}+\xi^2 , \\ s_{LT} &= -\frac{1}{\sqrt{2}}(1+\xi^2)^{1/2} , \\ s'_T &= \xi(1+\xi^2)^{1/2} , \\ s'_{LT} &= -\frac{1}{\sqrt{2}}\xi , \end{aligned} \tag{96}$$

where $\xi=(q_L/Q)\tan\frac{1}{2}\theta$. The quantity $d\Sigma$ is

$$\begin{aligned} d\Sigma|_{\text{c.m.}} &= p_1 d\Omega_1 , \\ d\Sigma|_{\text{lab}} &= p_L d\Omega_L r . \end{aligned} \tag{97}$$

Hence the advantage of Eq. (95) is that it uses covariant structure functions $\tilde{R}$, and combines the c.m. and lab results into one formula—the only difference being the choice of $d\Sigma$ given in Eq. (97).

Finally, we address the question of how the hadronic spin variables are affected by the choice of frame for the hadronic current, item (iii) above. First, note that the boost (20) will not affect the deuteron helicity, since it is colinear with the deuteron momentum. However, since the momenta of the final-state nucleons are in general not colinear with the boost, the boost will introduce a precession (a Wigner rotation) of the nucleon spins through an angle θ_w about the axis $\mathbf{q}\times\mathbf{p}$, which is perpendicular to the plane defined by the direction of the boost ($\mathbf{q}$) and the three momentum of the particle ($\mathbf{p}$). This plane is just the ejectile plane defined in Fig. 2, and hence the boost will rotate the nucleon spins in this plane and therefore mix the l and s components of nucleon polarization. The amplitudes in the third and fourth columns of Tables X–XII will mix. The sizes of these terms will be frame dependent, but the structure of the results given in Tables X—XII will also hold for observables in the lab system. Hence the general conclusions of this paper (including the discussion of Sec. III) do not depend on which frame is used for the hadronic variables; only dynamical calculations of these quantities depend on the frame. The details of the Wigner rotation will be presented elsewhere.

We now turn to a discussion of possible programs of complete measurements.

III. COMPLETE SEPARATIONS

A. Introduction

Complete determination of photonuclear processes has been attempted in several different ways. We have adopted the method of Barker *et al.*[4] (for criticism of other approaches see this reference). We looked for a set of new amplitudes which made the separation obvious. The hybrid amplitudes presented in the preceding section accomplished this, just as in pion photoproduction. As we saw in Tables X–XII the structure functions became particularly simple when expressed in terms of the g_i. They become real and imaginary parts of bilinear combinations of $g_i's$. This form makes it comparatively easy to study what measurements are necessary in order to completely and uniquely determine all the complex amplitudes, as will be shown below.

Consider a simple example of the electrodisintegration of a spinless nucleus into two spinless fragments [^{4}He$(e,e'\pi^\circ)^4$He, for example]. There are only two independent helicity amplitudes, $J_0=|J_0|e^{i\phi_0}$ and $J_+=|J_+|e^{i\phi_+}$, and only five nonvanishing structure functions (only four of which are different):

$$\begin{aligned} R_L &= \eta^2\kappa^2|J_0|^2 , \\ R_T &= 2\kappa^2|J_+|^2 , \\ R_{TT}^{(\mathrm{I})} &= 2\kappa^2\mathrm{Re}(J_+J_-^*) = -R_T , \\ R_{LT}^{(\mathrm{I})} &= 4\eta\kappa^2\mathrm{Re}(J_0J_+^*) , \\ R_{LT'}^{(\mathrm{I})} &= 4\eta\kappa^2\mathrm{Im}(J_0J_+^*) , \end{aligned} \tag{98}$$

but there are only three independent observables: $|J_0|, |J_+|, \phi_{0+}=(\phi_0-\phi_+)$. The overall (absolute) phase is not an observable.

If we measure R_L, R_T, and one of the R_{LT}, we still cannot determine ϕ_{0+} unambiguously. For example, a measurement of R_{LT} will determine $\cos\phi_{0+}$, which gives ϕ_{0+} in the first or fourth quadrant if it is positive, and in the second or third quadrant if it is negative. A similar ambiguity results if only $R_{LT'}$, which determines $\sin\phi_{0+}$, is measured. To completely remove the ambiguity both of the "paired" amplitudes (R_{LT} and $R_{LT'}$) must be measured. But this measurement will also give the product $|J_0||J_+|$, requiring the measurement of only *one* other modulus to completely and unambiguously determine the three independent observables. This last measurement can be either R_L or $R_T(=-R_{TT})$. The program requiring the *fewest number* of measurements is therefore one in which "paired" amplitudes, together with a few "moduli," are measured.

Unfortunately, measurements of "paired amplitudes" will generally be more difficult, as they usually involve polarization observables. The best experimental program may well be to measure "moduli" if they are easy, and "paired" amplitudes as needed to eliminate ambiguities.

B. Overview of separation strategies

We begin the discussion of separation strategies by seeing what can be learned from the "paired" observables $(R_{LT}^{(\mathrm{I})},R_{LT'}^{(\mathrm{I})})$, $(R_{LT'}^{(\mathrm{II})},R_{LT}^{(\mathrm{II})})$, and $(R_{T'},R_{TT}^{(\mathrm{II})})$ detailed in Tables X and XII. If *all* the observables in Table X were measured, the complex amplitudes a_i, b_i, c_i, d_i, e_i, and f_i would all be determined uniquely, and hence the products of the g's which they contain. There are 18 different products of $g's$ which are so determined, and these fall into two separate classes, as shown in the two left-hand columns of Table XIII. No product of an amplitude from class A times an amplitude from class B is present (and of course there are no products of the first six amplitudes with each other, nor the last six with each other). Hence, there are terms like $g_1^*g_{13}$ and $g_1^*g_{16}$, but no term like $g_1^*g_{14}$. From $g_1^*g_{13}$ and $g_1^*g_{16}$, one can determine

TABLE XIII. Products $g_i^* g_j$ which can be determined from measurements of the six observables detailed in Tables X and XII. In each case, a complete set of measurements determines only the nine pairs of products involving the upper three g^*'s with the lowest three g's in class A, and a similar nine pairs of products in class B.

$(R_{LT}^{(I)}, R_{LT'}^{(I)})$		$(R_{T'}, R_{TT}^{(II)})$		$(R_{LT'}^{(II)}, R_{LT}^{(II)})$	
Class A	Class B	Class A	Class B	Class A	Class B
g_1^*	g_2^*	g_7^*	g_8^*	g_7^*	g_8^*
g_4^*	g_3^*	g_{10}^*	g_9^*	g_{10}^*	g_9^*
g_5^*	g_6^*	g_{11}^*	g_{12}^*	g_{11}^*	g_{12}^*
. . .	. . .	. . .	. . .	. . .	. . .
g_{13}	g_{14}	g_1	g_2	g_{13}	g_{14}
g_{16}	g_{15}	g_4	g_3	g_{16}	g_{15}
g_{17}	g_{18}	g_5	g_6	g_{17}	g_{18}

$|g_1||g_{13}|$, $|g_1||g_{16}|$, $\phi_1-\phi_{13}$, and $\phi_1-\phi_{16}$, from which the relative size of $|g_{13}|$ and $|g_{16}|$ can be deduced, and $\phi_{13}-\phi_{16}$. In a similar manner the phase difference between all amplitudes in each class can be determined, but the overall phase difference between the two classes remains undetermined. Also, two moduli cannot be determined, which could be taken to be $|g_1|$ and $|g_2|$ (if these are assumed, all other moduli are fixed). Hence, of the 23 possible observables associated with the amplitudes which contribute to Table X, only 20 can be determined by the 36 possible measurements. Three cannot be determined.

The same analysis works for the other paired amplitudes $(R_{LT'}^{(II)}, R_{LT}^{(II)})$ and $(R_{T'}, R_{TT}^{(II)})$ of Table XII. The classes of amplitudes are displayed in the four rightmost columns of Table XIII. Note that the combination of *all* of these measurements still leaves the same three observables undetermined. The two classes of amplitudes are enlarged, but there is no mixing which would determine the missing moduli or phase. The expanded classes are

$$A: \{g_1 g_4 g_5 g_7 g_{10} g_{11} g_{13} g_{16} g_{17}\}, \qquad B: \{g_2 g_3 g_6 g_8 g_9 g_{12} g_{14} g_{15} g_{18}\}. \tag{99}$$

Furthermore, the additional measurements are less efficient in adding new information. If all of the products of amplitudes from a given "paired" set were known, for example, the measurements of the next "paired" set would add only 12 new observables, and measurements of the last pair would add no new information. This shows that care must be taken to plan experimental programs optimally.

The missing moduli, one from class A and one from class B, can be determined by two measurments from Table XI. A convenient choice would be two of the unpolarized observables R_L and $R_T^{\pm}$. However, no measurement involving any combination of polarized electron beam, polarized deuteron target, or polarized recoil proton can determine the last phase. For this, at least one measurement of neutron recoil polarization is needed. Recall that the neutron observables are identical to the proton observables except for the interchange of $g_1 \leftrightarrow g_2$, $g_5 \leftrightarrow g_6$, $g_9 \leftrightarrow g_{10}$, $g_{13} \leftrightarrow g_{14}$, and $g_{17} \leftrightarrow g_{18}$. This mixes up the classes in Eq. (99), making it possible to determine the last relative phase. However, only measurments which depend on this phase can be used for this purpose. It turns out that only the observables which depend on P_s' and P_l' (e_i and f_i in Table X, a_i, b_i, c_i, and d_i in Table XII, and α_i and β_i in Table XI) are satisfactory—the others are not sensitive to this interchange.

Our discussion has shown that at least one neutron recoil polarization measurement is essential to a complete determination of the 18 deuteron electrodisintegration hybrid amplitudes, and that this must involve measuring P_l' or P_s'. If this measurement is to be made with an unpolarized deuteron target, then the quantities must be chosen from $R_{LT'}(s')$, $R_{LT'}(l')$, $R_{T'}(s')$, $R_{T'}(l')$, $R_{LT}(s')$, $R_{LT}(l')$, $R_{TT}(s')$, or $R_{TT}(l')$, where the prime on the s or l argument signifies a neutron polarization measurement.

We have focused on proton polarization measurements in this section, assuming that such measurements would be easier to carry out experimentally. One can readily see, however, that there is a correspondence between proton and neutron polarization measurements, and the best strategy could well be to use a number of both.

At this point a number of questions arise concerning the "best" methods for separating the 18 amplitudes. We believe that we have provided sufficient detail for the reader to work out his own preferred strategy, and will not pursue discussion of the subject here.

IV. CONCLUSIONS

This paper analyzes the differential cross section for the process $d(e,e'p)n$ in which the scattered electron and the recoil proton are measured in coincidence. The cross section can be expressed in terms of nine (unknown) hadronic structure functions defined in Table III. If the hadronic structure functions are expressed in terms of variables defined in the center of mass (c.m.) of the outgoing hadrons, the relevant formula is Eq. (30). If lab variables are used, the expression given in Eq. (94) is appropriate. Equation (95) gives a formula convenient in either frame.

Each of the nine structure functions can depend on the polarization of the deuteron target, and/or the polarization of the recoil proton. If all possible combinations of polarizations are considered, each of the nine structure functions depend on 18 independent observables, for a total of $9\times 18=162$ observables. The dependence of these observables on the 18 independent complex helicity am-

plitudes which completely describe deuteron electrodisintegration is given in Tables X–XII. The 18 hybrid amplitudes g_i are linear combinations of the 18 helicity amplitudes, given explicitly in the Appendix, or in general terms in Eqs. (66) and (67).

Even though there are 162 observables in Tables X–XII, it is shown in Sec. III that these are not sufficient to determine all of the 35 real functions implied by the existence of the 18 complex helicity amplitudes. One phase, relating the two classes of amplitudes given in Eq. (99), can only be obtained by measuring the polarization of the outgoing neutron. Dynamical calculations of these observables are planned for future work.

ACKNOWLEDGMENTS

It is a pleasure to acknowledge helpful conversations with T. W. Donnelly, who first interested us in this problem. M. Moravcsik helped us understand some of our early results, so that we could recast the final results in the simplified form presented here. Lectures by J. D. Walecka were also helpful in the early stages of this work. Support by the Department of Energy, under Grant No. DE-FG05-88ER40435 is gratefully acknowledged.

APPENDIX

The connection, Eqs. (66) and (67), between the hybrid amplitudes g_i used in this paper, and the helicity amplitudes F_i defined in Eq. (51) can be summarized by the matrix relations

$$g_i = \Lambda_{ij} F_j \ , \tag{A1}$$

where, for transverse amplitudes ($i,j=1$–12),

$$\Lambda_{ij} = \frac{1}{4} \begin{pmatrix}
i & i & \sqrt{2} & \sqrt{2} & -i & -i & 1 & -1 & -i\sqrt{2} & i\sqrt{2} & -1 & 1 \\
i & i & \sqrt{2} & \sqrt{2} & -i & -i & -1 & 1 & i\sqrt{2} & -i\sqrt{2} & 1 & -1 \\
-i\sqrt{2} & i\sqrt{2} & 0 & 0 & -i\sqrt{2} & i\sqrt{2} & \sqrt{2} & \sqrt{2} & 0 & 0 & \sqrt{2} & \sqrt{2} \\
i\sqrt{2} & -i\sqrt{2} & 0 & 0 & i\sqrt{2} & -i\sqrt{2} & \sqrt{2} & \sqrt{2} & 0 & 0 & \sqrt{2} & \sqrt{2} \\
-i & -i & \sqrt{2} & \sqrt{2} & i & i & -1 & 1 & -i\sqrt{2} & i\sqrt{2} & 1 & -1 \\
-i & -i & \sqrt{2} & \sqrt{2} & i & i & 1 & -1 & i\sqrt{2} & -i\sqrt{2} & -1 & 1 \\
-1 & 1 & i\sqrt{2} & -i\sqrt{2} & 1 & -1 & i & i & \sqrt{2} & \sqrt{2} & -i & -i \\
1 & -1 & -i\sqrt{2} & i\sqrt{2} & -1 & 1 & i & i & \sqrt{2} & \sqrt{2} & -i & -i \\
\sqrt{2} & \sqrt{2} & 0 & 0 & \sqrt{2} & \sqrt{2} & i\sqrt{2} & -i\sqrt{2} & 0 & 0 & i\sqrt{2} & -i\sqrt{2} \\
\sqrt{2} & \sqrt{2} & 0 & 0 & \sqrt{2} & \sqrt{2} & -i\sqrt{2} & i\sqrt{2} & 0 & 0 & -i\sqrt{2} & i\sqrt{2} \\
1 & -1 & i\sqrt{2} & -i\sqrt{2} & -1 & 1 & -i & -i & \sqrt{2} & \sqrt{2} & i & i \\
-1 & 1 & -i\sqrt{2} & i\sqrt{2} & 1 & -1 & -i & -i & \sqrt{2} & \sqrt{2} & i & i
\end{pmatrix} , \tag{A2}$$

while, for longitudinal amplitudes ($i,j=13$–18),

$$\Lambda_{ij} = \frac{1}{2} \begin{pmatrix}
i & \sqrt{2} & -i & -1 & i\sqrt{2} & 1 \\
i & \sqrt{2} & -i & 1 & -i\sqrt{2} & -1 \\
-i\sqrt{2} & 0 & -i\sqrt{2} & \sqrt{2} & 0 & \sqrt{2} \\
i\sqrt{2} & 0 & i\sqrt{2} & \sqrt{2} & 0 & \sqrt{2} \\
-i & \sqrt{2} & i & 1 & i\sqrt{2} & -1 \\
-i & \sqrt{2} & i & -1 & -i\sqrt{2} & 1
\end{pmatrix} . \tag{A3}$$

[1] T. W. Donnelly, in *New Vistas in Electro-Nuclear Physics*, edited by E. L. Tomusiak, H. S. Caplan, and E. T. Dressler (Plenum, New York, 1985); and in *Proceedings of the CEBAF 1985 Summer Workshop*, edited by H. Crannell and F. Gross (CEBAF, Newport News, Virginia, 1985), p. 57; A. S. Raskin and T. W. Donnelly, Ann. Phys. (N.Y.) **191**, 78 (1989).

[2] H. Arenhövel, W. Leidemann, and E. L. Tomusiak, Z. Phys. A **331**, 123 (1988), and references therein; H. Arenhövel, Few Body Systems **4**, 55 (1988).

[3] V. Dmitrasinovic, T. W. Donnelly, and Franz Gross, *Research Program at CEBAF (III), RPAC III*, edited by F. Gross (CEBAF, Newport News, Virginia, 1988), p. 547; *Report of the CEBAF Out-of-Plane Task Force* (CEBAF, Newport News, Virgnia, 1988), p. 183, in RPAC III.

[4] I. S. Barker, A. Donnachie, and J. K. Storrow, Nucl. Phys. **B95**, 347 (1975).

[5] G. R. Goldstein and M. J. Moravcsik, Nucl. Instrum. Methods A **240**, 43 (1985).

[6] F. M. Renard, J. Tran Thanh Van, and M. LeBellac, Nuovo Cimento **38**, 552 (1965).

[7] J. D. Walecka and P. A. Zucker, Phys. Rev. **167**, 1479 (1968).

[8] W. Fabian and H. Arenhövel, Nucl. Phys. **A314**, 253 (1979).

[9] G. G. Ohlsen, Rep. Prog. Phys. **35**, 717 (1972).

[10] M. Jacob and G. C. Wick, Ann. Phys. (N.Y.) **7**, 404 (1959).

[11] Although the phase η_g is not explicitly stated in Ref. 6, it can be unambiguously determined from their result for the proton recoil polarization observables. The change of sign of η_g induces the following change in the observables: $R_{TT}^{(\mathrm{I,II})} \rightarrow -R_{TT}^{(\mathrm{I,II})}$; $R_{LT}^{(\mathrm{I,II})} \leftrightarrow -R_{LT'}^{(\mathrm{II,I})}$. An explicit calculation of these observables shows that Rènard *et al.* used $\eta_g = -1$.

[12] A. Kotanski, Acta Phys. Pol. **29**, 699 (1966); **30**, 629 (1966).

[13] C. N. Papanicolas *et al.*, University of Illinois report.

[14] N. Christ and T. D. Lee, Phys. Rev. **143**, 1310 (1966).